npj | heritage science

Article

https://doi.org/10.1038/s40494-025-01676-0

Archaeometallurgical analysis of early Qin bronze thin sheets from Shaanxi China

Ruoxi Huang[1], Cheng Liu[1] ✉, Xue Ling[1], Yuan He[1], Linhan Xue[1,2] & Yun Liang[1] ✉

This research conducted a comprehensive scientific analysis of early Spring and Autumn period bronze thin sheets (coffin decorations) excavated from the Weijiaya site in Shaanxi, China, a significant archaeological site for early Qin culture. By employing microscopic observation, X-ray diffraction (XRD), micro X-ray fluorescence (μXRF) mapping, metallurgical microscopy and scanning electron microscopy–energy dispersive X-ray spectroscopy (SEM–EDS), this study investigated the corrosion patterns, metallurgical structures and alloy compositions of these bronzes. Our findings indicate that the bronze thin sheets were forged from low-tin bronze, with tin contents ranging from 5.71% to 14.01%. Predominant corrosion products include cassiterite, cerussite, malachite, cuprite and tenorite. Comparisons with contemporary bronzes from Henan, Shannxi, Shanxi, Hubei and Gansu reveal both similarities and regional differences in manufacturing techniques, highlighting early Qin's technological advancements and cultural exchanges. This research provides new insights into early Qin culture and ancient Chinese bronze metallurgy.

The Qin dynasty marked a pivotal period in the history of Chinese civilisation, representing the first multiethnic, centralised feudal empire, which laid the foundation for China's unification and development. Qin culture served as a pivotal bridge in historical development, assimilating the cultural essence of the Shang and Zhou periods while laying the groundwork for the cultural advancements of the Han and Tang dynasties. Thus, it constitutes an indispensable part of Chinese cultural heritage.

The early Qin people resided in what is now southeastern Gansu Province, China. Through integrations with the Han, Di, Qiang and Xirong ethnic groups, they formed a distinct Qin ethnic identity. Throughout its expansion and strengthening, Qin undertook multiple capital relocations to meet the demands of political, military and economic development. This journey began at the earliest capital of Xiquanqiu and moved through successive capitals such as Qinyi, Qianyi, Qianweizhihui, Pingyang, Yongcheng, Jingyang and Liuyang, finally settling in Xianyang. The archaeological site at Weijiaya, located at the intersection of the Qianhe River and the Weihe River in the Baoji area of Shaanxi Province, China, is situated on a gentle slope that transitions from the loess plateau to the riverbank terraces, with higher terrain in the Northeast and lower terrain in Southwest China. This site spans Weijiaya, Chenjiaya and Fengjiazui villages and is considered the likely location of the ancient capital "*Qianweizhihui*" (as shown in Fig. 1). From 2021, investigations, surveys, and excavations were conducted at the Weijiaya site by Northwest University and other institutions. The discoveries included well-preserved city wall remains and two high-status noble tombs (M2 and M4) from the early Spring and Autumn periods. In Tomb M2, numerous fragmented bronze thin sheets (coffin decorations) were excavated and restored into four bronze *Sha*-decorations (M2: 36, M2: 37, M2: 38 and M2: 39) and eight single *Shajiao*-decorations (M2: 40, M2: 41, M2: 58, M2: 107, M2:117, M2:122, M2:157 and M2: 158). These were symmetrically placed between the inner and outer coffins, with one single *Shajiao*-decoration positioned at each corner of the outer coffin chamber and beside each bronze *Sha*-decoration[1]. For convenience in writing, it will be referred to as *Sha* and single *Shajiao* in the following text.

As a type of significant funerary object, *Sha* was predominantly used from the late Western Zhou to the early Spring and Autumn period, primarily among the noble class, embodying distinct ritualistic characteristics. *Sha* is made from various materials, including bamboo, wood, feathers and bronze. It served as a ceremonial accessory during funerals, as part of the coffin decorations, and was carried alongside the coffin to shield it during the procession[2]. In the early Spring and Autumn Qin tombs at Weijiaya, bronze *Sha* were symmetrically positioned between the inner and outer coffins. This practice aligns with the customary practice of positioning bronze *Sha* on the inner coffin or around it. The quantity of *Sha* is closely tied to the tomb owner's status. An emperor would be buried in seven months with eight layers of *Sha*, a feudal lord in five months with six *Sha*, and a high official in three months with four *Sha*[3]. The tomb M2 yielded four bronze *Sha* and eight single *Shajiao*, suggesting that the tomb belonged to a high official, as corroborated by the simultaneous discovery of five bronze dings.

[1]School of Cultural Heritage, Northwest University, No. 1 Xuefu Avenue, Xi'an, 710127, China. [2]Shaanxi Academy of Archaeology, No. 2999 Zhongnan Avenue, Xi'an, 710109, China. ✉e-mail: liucheng@nwu.edu.cn; yunl2002@126.com

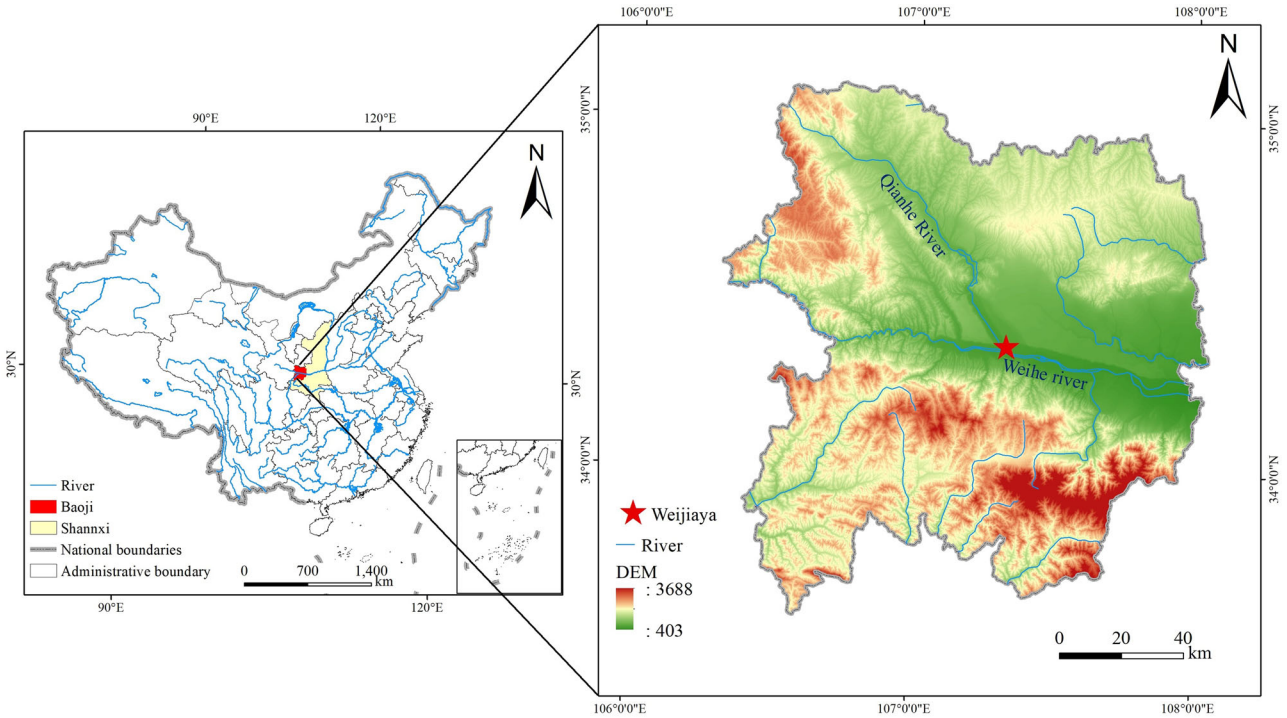

Fig. 1 | The geographical location of the Weijiaya site in Shaanxi, China.

Since the 1950s, distinctive bronze pieces shaped like the Chinese character "mountain" have been frequently unearthed in Zhou dynasty tombs across Shaanxi, Henan, Gansu, Shanxi and Shandong, China[3–5]. In 2006, Wang and others confirmed through literature and archaeological evidence that these "mountain-shaped" pieces were indeed bronze *Sha*[2]. The bronze *Sha* was crafted either by casting or hot-working. The monolithic *Sha* was cast in one piece, whereas the hot-worked *Sha* was assembled from separate parts via bronze sheets or nails for joining[3]. The production of sectional *Sha* relies on the development of forging technology. The popularity of bronze *Sha* coincided with the rapid advancement of hot-worked, thin-walled bronze technology. Li defined hot-worked, thin-walled bronzes as those with a wall thickness between 0.5–1.5 mm, typically produced via low-tin hot-working (tin content below 17%, working temperature of 200–300 °C) or high-tin hot-working (tin content above 17%, temperature of 500–700 °C), with most artefacts formed through low-tin hot-working[6]. The bronze *Sha* samples tested in this paper all conform to this definition.

Research on Chinese hot-worked, thin-walled bronzes began in the 1980s. Goodway and others conducted scientific tests on various types of ancient Chinese gongs, hypothesising that they were hot-worked and then quenched[7]. The earliest discovered hot-worked, thin-walled bronzes were from the Gamatai tomb in Qinghai, dating to the late Qijia culture[8]. Prior to the middle Western Zhou, such artefacts were rare, and were found mainly in the Northwest and Central Plains regions. Zhang conducted technological tests on bronzes from a Western Zhou tomb in Gansu's Yujiawan, finding that three were made from a ternary alloy of copper, tin and lead; and one from a binary copper-tin alloy, with tin contents ranging from 12.4 to 16.2%, lead contents under 6%, and thicknesses between 0.51 and 1.26 mm[9]. From the middle to late Western Zhou through the Spring and Autumn period, the use of hot-worked, thin-walled bronzes gradually increased, expanding to regions along the middle Yangtze River, the Southwest and North China. For example, Shao analysed two coffin decorations from Gansu's Dabuzishan site, showing that they were made from a ternary copper-tin-lead alloy via hot-working, with a tin content of 16% and lead content of 3.2%[4]. Li analysed a batch of decorative pieces unearthed in Xiaxiangpu tomb in Henan, and reported that they were tin bronze, the metallographic structure was hot-worked and cold-worked, and the tin content was 7.76%-12.81%[6]. At present, research on hot-worked, thin-walled bronzes has focused on the production process. There remains a lack of organised research and analysis on hot-worked, thin-walled bronzes unearthed in different regions, particularly concerning their temporal and spatial distributions, development history and motivations behind their creation. In-depth research is needed to understand the application and development of this technology in early Qin culture.

Current studies on bronze *Sha* have focused primarily on traditional archaeological analyses, with fewer conducted through the lens of archaeological science. Systematic scientific analyses have been conducted only on *Sha* from Shaanxi's Liujiawa site and Shanxi's Yangshe tomb (Dabuzishan tomb in Gansu Province, also unearthed suspected bronze coffin decorations)[3–5]. Discussions on the corrosion characteristics of bronze *Sha* and their impact on production techniques are almost nonexistent. The bronze *Sha* unearthed from the Weijiaya site was some of the earliest and best-preserved from Qin culture. This study conducted a scientific investigation into the corrosion features, alloy composition and manufacturing techniques of bronze *Sha* from the Weijiaya site. By comparing them with bronze *Sha* from other sites, we can explore the development of hot-working techniques during the early Qin culture and the exchange of hot-worked, thin-walled bronze production techniques between regions from late Western Zhou to the early Spring and Autumn period. This research could deepen our understanding of the bronze artefacts of early Qin culture and enrich the study of ancient Chinese hot-worked, thin-walled bronze techniques.

Methods

In this study, samples from bronze *Sha* and single *Shajiao* unearthed from Tomb M2 at the Weijiaya site in Baoji, Shaanxi, China, were analysed (Fig. 2). The bronze *Sha* (M2: 36, M2: 37, M2: 38 and M2: 39) are shaped like the Chinese character for "mountain". Each bronze *Sha* features a central sharp-pointed long bronze piece called *Shagui* standing vertically, with the side *Shajiao* resembling birds. The birds face outwards, the tails face each other, the crests curl backwards, and the bodies have slender, curled tails. The single *Shajiao* (M2: 40, M2: 41, M2: 58, M2: 107, M2:117, M2:122, M2:157 and M2: 158) are shaped like phoenix birds, with outwards facing

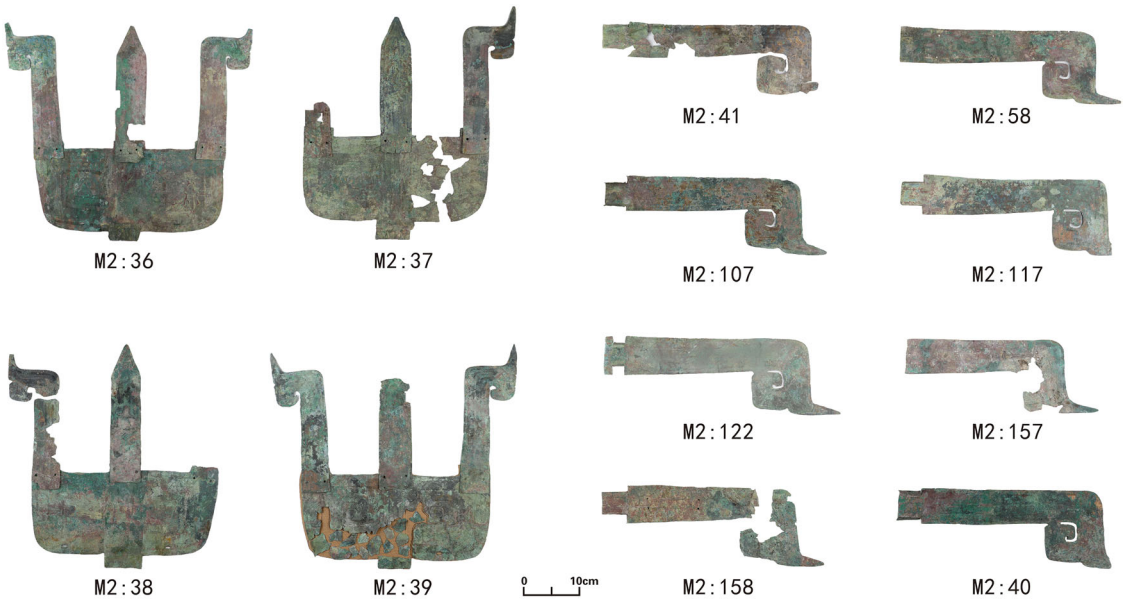

Fig. 2 | The excavated bronze *Sha* (M2: 36, M2: 37, M2: 38 and M2: 39) and single *Shajiao* (M2: 36, M2: 37, M2: 38 and M2: 39).

heads, partially damaged crests, slender curled tails and hollowed beak areas, approximately the same size as each other.

Both the bronze *Sha* and single *Shajiao* feature impressed patterns on their surfaces. The surface of *Shagui* is impressed with two broad lines corresponding to the contour, whereas the side *Shajiao* has four narrower parallel lines corresponding to their contours, and the base called *Shashou* features symmetrical phoenix bird patterns. The single *Shajiao*, shaped like phoenix birds similar to the side *Shajiao* of the bronze *Sha*, are impressed with four parallel lines matching their contours, with an upper part featuring a hollow curled pattern[1].

Microsampling was conducted on some of the metal artefacts. The sampling method used was water-cooled cutting; some samples were fine fragments detached naturally during the restoration process and some were rust powder from severely corroded samples. Sampling followed the principle of minimal intervention, with details provided in Supplementary Data 1: Table S1.

Microscopic observation

The microscopic corrosion features, local craftsmanship details and surface ornamentation of the samples were observed via an OLYMPUS TG-7 optical microscope camera for on-site photography.

Metallographic observation

The instrument used was a ZEISS Axio Scope A1 metallographic microscope. The samples were first embedded in a cross-section using Araldite AB epoxy resin. They were then ground and polished with various grades of sandpaper and polishing cloths. The samples were then etched for 1–3 s using a ferric chloride hydrochloric acid: solution (reagent ratio of ethanol: hydrochloric acid solution: ferric chloride = 12:3:1) and subsequently observed under the metallographic microscope.

Scanning electron microscopy–energy dispersive X-ray spectroscopy (SEM–EDS)

The samples were polished again, carbon-coated, and analysed via a TESCAN VEQA-3XMU scanning electron microscope and an OXFORD INCAx-act X-ray energy spectrometer for micromorphology observation and composition analysis. Before each test, a pure copper sheet was used for optimal calibration. Considering the segregation in bronze samples, five regions were selected from each sample for elemental analysis, with the average value representing the sample's compositional elements. The test conditions included a tungsten filament electron gun, a backscatter probe, an excitation voltage of 20 kV, a scanning time of 60 s, and a working distance of 15 mm. The total content of the raw data was between 95 and 105%; all the data were normalised and presented as mass fractions.

X-ray diffraction analysis (XRD)

Phase analysis of the corrosion powders was conducted using a German Bruker D8 Advance X-ray diffractometer. The test conditions were as follows: an operating voltage of 40 kV, an operating current of 100 mA, a scanning angle range of 5°–90°, and a scanning speed of 5°/min. The spectra obtained were analysed via Jade 6.0 software. Micro X-ray fluorescence (μXRF) mapping The experimental equipment used was a Bruker M4 TORNADO PLUS micro-XRF instrument, which performed micro-XRF mapping analysis on some samples. With the help of multicapillary focusing and an aperture management system, M4 provides a minimum spot size of 20 μm. Combined with its high-speed large sample stage and ESPRIT analysis software, it offers more flexible and precise results for in situ nondestructive analysis of cultural artefacts. Other testing conditions included a dual silicon drift detector (SDD), a rhodium target, an operating voltage of 50 kV, an operating current of 600 μA and a vacuum optical path.

Results

Microscopic observation results

Microscopic observations (Fig. 3) reveal linear engraved traces at the decorated areas, with some lines intersecting, starting either sharply or in a blunt rounded fashion. Clear bends and pauses are observed at the junctions of patterns. Cut marks are present along the edges of the artefacts and within the openwork patterns. Both the entire surface of the bronze Sha and the single *Shajiao* exhibit distinct polishing lines that are arranged neatly and are almost uniformly spaced. The *Shagui*, *Shashou* and left and right *Shajiao* of the bronze *Sha*, as well as some single *Shajiao*, all have nearly circular borings, with the surrounding metal recessing towards the back.

Elemental composition analysis results

The SEM-EDS testing results are shown in Table 1. A value of 2% is used as the threshold to differentiate between alloy elements and impurity elements[10]. The majority of the 22 samples tested were copper-tin alloys (Cu-Sn), with tin contents ranging from 5.71 to 14.01%. Ancient tin bronzes are divided into high-tin and low-tin types. Bronzes with tin content less than less than 17% are considered low-tin, whereas those with tin content

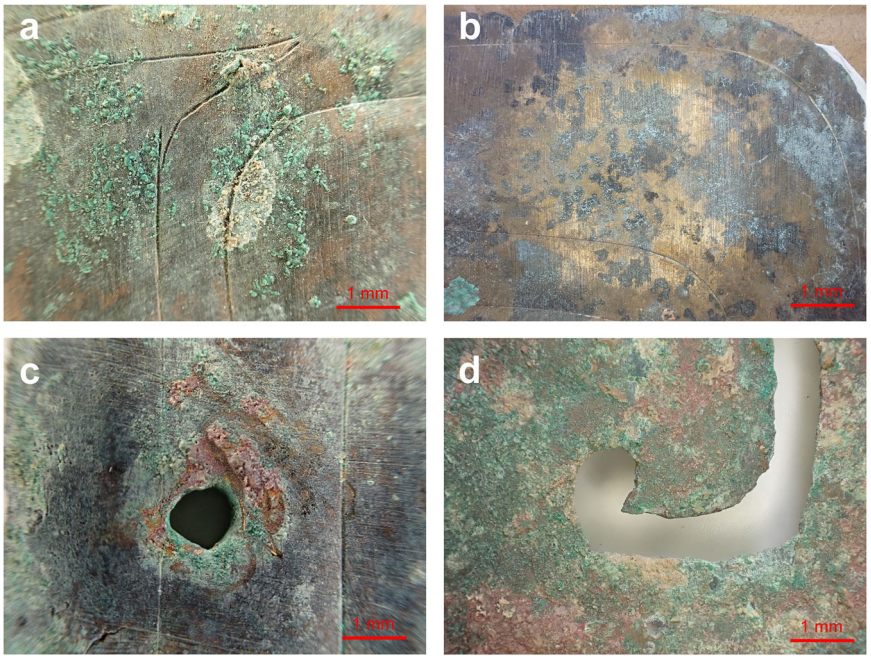

Fig. 3 | Microscopy images of *Sha* and single *Shajiao*. **a** Engraved marks on the upper right corner of M2:117 single *Shajiao*; **b** Polishing marks of M2:117 single *Shajiao*; **c** A boring of M2:38 bronze *Sha*'s left *Shajiao*; **d** Cut marks at the hollowed-out areas of M2:40 single *Shajiao*.

Table 1 | SEM–EDS analysis results of bronze *Sha* and single *Shajiao*, in wt%, reporting the average of multiple analyses per sample; "others" represent the total amounts of As, Ni, Ag, Zn, Sb, Co, Bi, Au and Cl

Sample number	Archaeological number	Cu	Sn	Pb	O	S	Cl	Fe	Others
M2:38-1	M2:38	70.91	13.84	3.90	9.99	0.00	0.24	0.01	1.12
M2:38-2	M2:38	62.84	10.54	19.60	5.61	0.03	0.00	0.05	1.32
M2:38-3	M2:38	87.29	7.46	0.18	3.52	0.18	0.02	0.02	1.35
M2:37-1	M2:37	79.53	14.01	0.58	3.84	0.13	0.04	0.02	1.86
M2:37-2	M2:37	79.95	13.25	0.85	3.94	0.29	0.06	0.02	1.65
M2:39-1	M2:39	87.96	6.07	0.26	4.77	0.05	0.07	0.07	0.75
M2:39-2	M2:39	90.18	6.22	0.11	2.12	0.05	0.03	0.02	1.28
M2:39-3	M2:39	79.53	11.90	0.48	6.72	0.11	0.11	0.03	1.13
M2:39-4	M2:39	82.06	10.00	0.90	5.52	0.21	0.06	0.01	1.23
M2:41-1	M2:41	82.49	11.62	0.34	4.18	0.09	0.04	0.01	1.23
M2:41-2	M2:41	79.74	11.36	0.53	6.36	0.39	0.05	0.03	1.54
M2:41-3	M2:41	72.30	11.62	9.82	4.53	0.25	0.10	0.06	1.31
M2:41-4	M2:41	75.26	11.23	4.14	7.02	0.31	0.33	0.05	1.66
M2:41-5	M2:41	67.98	10.20	16.58	3.77	0.11	0.00	0.04	1.33
M2:40-1	M2:40	82.70	9.54	0.68	5.84	0.08	0.05	0.02	1.10
M2:40-2	M2:40	86.80	9.22	0.24	2.68	0.05	0.03	0.03	0.95
M2:158-1	M2:158	80.71	11.95	0.22	5.45	0.25	0.04	0.02	1.37
M2:158-2	M2:158	89.11	6.70	0.04	2.75	0.03	0.05	0.00	1.31
M2:158-3	M2:158	83.41	7.49	0.41	6.76	0.35	0.07	0.03	1.50
M2:158-4	M2:158	76.19	6.44	12.24	3.68	0.18	0.01	0.00	1.27
M2:157	M2:157	88.46	5.71	0.47	3.67	0.17	0.07	0.02	1.43
M2:107	M2:107	85.32	6.84	1.61	4.98	0.26	0.07	0.02	0.90

greater than 17% are considered high-tin[11]. The samples analysed in this study are low-tin bronzes. Six samples had high-lead contents, ranging from 3.90% to 19.60%.

The results of energy spectrum mapping (Fig. 4) show that, in addition to being uniformly distributed within the metal matrix in particulate and striated forms, lead is also concentrated at the edges of most samples where corrosion has occurred. This is likely due to the migration and accumulation of lead from the matrix due to corrosion[12]. The density of the lead distribution is proportional to the proximity to the edges in some samples. Tin is uniformly distributed throughout the interiors of the samples.

Metallographic microscopic observation results

Metallographic observations, as shown in Supplementary Data 2: Table S2 and Fig. 5, reveal that the metallographic structures of this

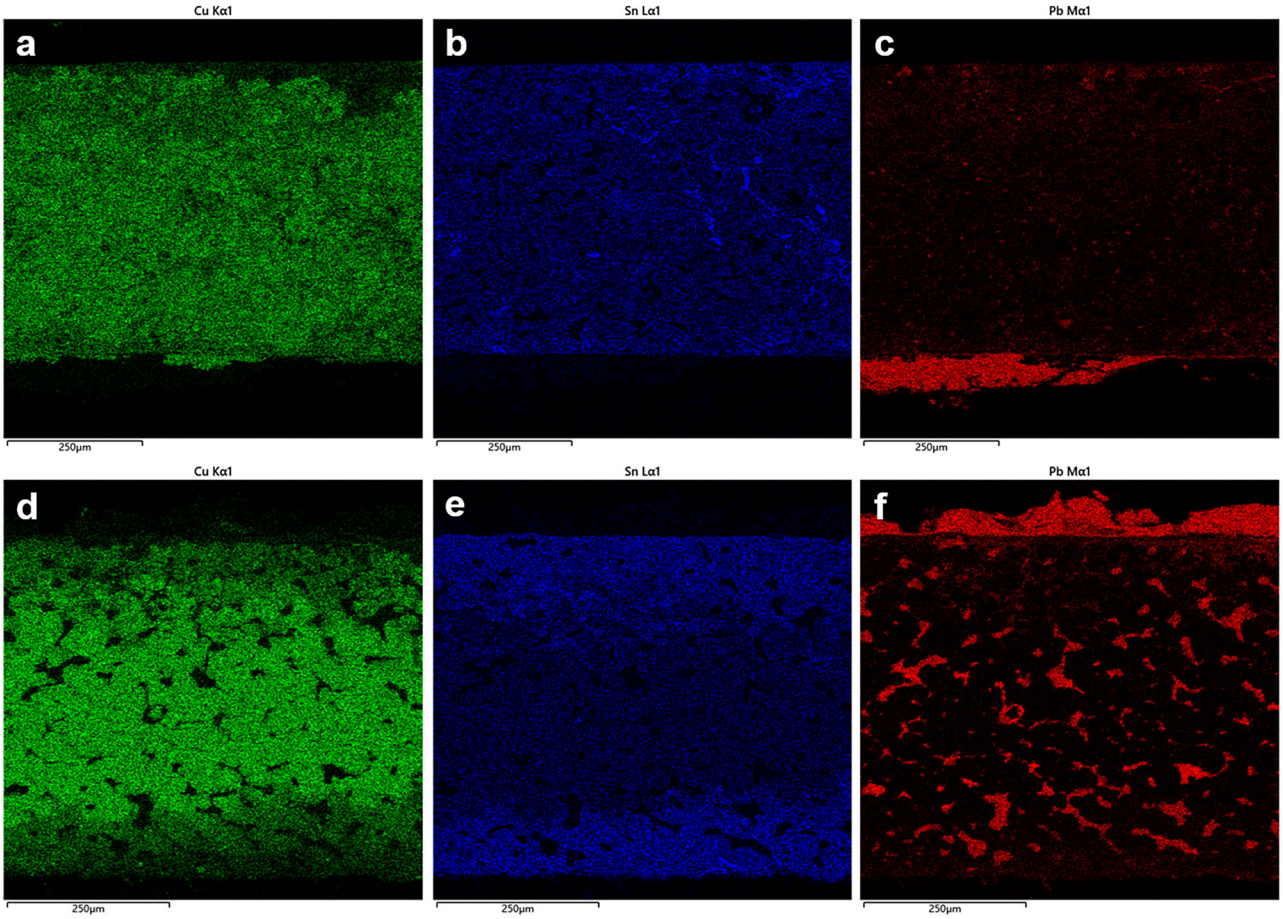

Fig. 4 | Energy spectrum maps of copper (Cu), tin (Sn) and lead (Pb) elements in some artefacts. a The Cu map of sample M2:38-1; **b** The Sn map of sample M2:38-1; **c** The Pb map of sample M2:38-1; **d** The Cu map of sample M2:38-2; **e** The Sn map of sample M2:38-2; **f** The Pb map of sample M2:38-2.

batch of bronze *Sha* and single *Shajiao* are all indicative of hot-worked structures. All the samples exhibit uniform recrystallised α solid solution grains and twins, with no (α + δ) eutectoids observed. Lead is evenly dispersed in small particles or large spheroids at the grain boundaries, and in some high-lead-content samples, lead particles are also distributed in bands between grain gaps. Spherical sulfide inclusions are visible at the grain boundaries in most samples. Among the 22 samples, six samples presented strain lines, which are indicative of cold working traces.

X-ray diffraction analysis results

X-ray diffraction analysis of various coloured corrosion products on each sample surface is presented in Supplementary Data 3: Table S3 and Fig. 6. The results indicate that the main corrosion products of bronze *Sha* and single *Shajiao* unearthed at the Weijiaya site include cassiterite (SnO_2), malachite [$Cu_2(OH)_2CO_3$], cerussite ($PbCO_3$), tenorite (CuO) and cuprite (Cu_2O). The main components of white, grey-white and yellow corrosion products are cerussite ($PbCO_3$) and cassiterite (SnO_2) or mixtures thereof. The black corrosion products are tenorite (CuO), some with small amounts of cassiterite (SnO_2). The red corrosion products are cuprite (Cu_2O) mixed with minor amounts of cerussite ($PbCO_3$). Some bronze surfaces exhibit light green powdery corrosion, mainly consisting of malachite [$Cu_2(OH)_2CO_3$], sometimes with cerussite ($PbCO_3$), and no harmful corrosion components, such as copper chlorides, are detected. Additionally, the green-yellow corrosion of bronze *Sha* M2:37 and single *Shajiao* M2:40 and M2:41 was identified as a mixture of pyromorphite [$Pb_5(PO_4)_3Cl$] and cerussite ($PbCO_3$).

Micro X-ray fluorescence (μXRF) mapping results

Micro X-ray fluorescence (μXRF) mapping is conducted on some samples. Single-element μ-XRF maps are shown in Fig. 7 (maps for elements at low concentrations are blurry because of interference from other elements). The distribution results of copper (Cu), tin (Sn) and lead (Pb) in the unearthed bronze *Sha* from the Weijiaya site are uneven. In deep green, black and red areas, the copper content is greater than that in earthy yellow, reddish-brown and white areas; lead-rich areas typically appear white to grey.

Discussion

The distributions of corrosion products on the bronze *Sha* and single *Shajiao* is uneven. Combining the XRD analysis and μXRF mapping results, it is evident that the main phases in the dark green areas are malachite, those in the black areas are tenorite, and those in the red areas are cuprite, with yellow, white, reddish-brown and earth yellow areas primarily containing cassiterite and cerussite. A rare corrosion product, pyromorphite, is also identified. This product has been discovered at archaeological sites such as San Polo d'Enza in Italy; the coastal area of Tarros in Sardinia, Italy; and the Lijiaba and Yujiaba sites in Chongqing, China[13–15]. Since the bronze *Sha* and single *Shajiao* were placed between the inner and outer coffins, we assume that pyromorphite formed due to the influence of phosphates from the bones of the tomb owner and the dogs sacrificed at the southeast corner of the second tier[16].

During the corrosion process, the forms of metal elements present are influenced by the specific burial environment[17–21]. Previous research on the soil burial conditions in the Guanzhong area of Shaanxi, China, where the Weijiaya site is located, revealed that the environment is characterised by alkaline, low-chloride conditions[22]. In this environment, the likelihood of

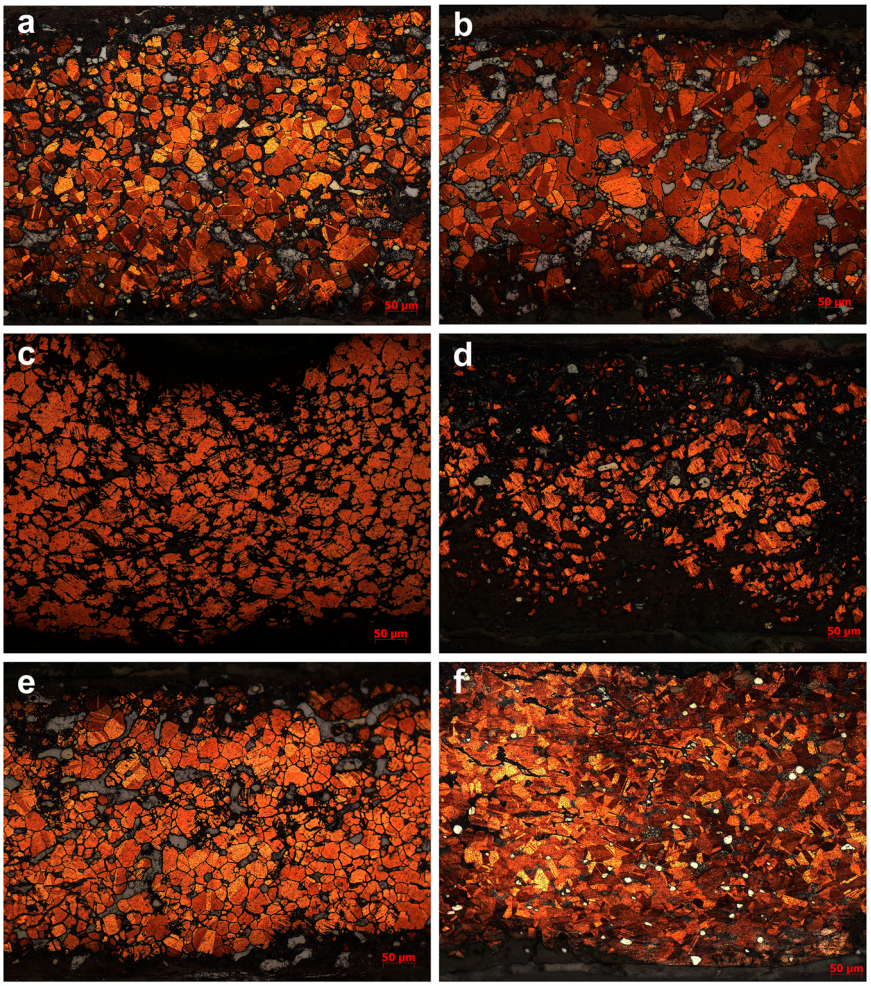

Fig. 5 | Metallographic micrographs of some samples. a Metallographic micrograph of M2:37-1 (from the middle lower area of *Shashou* with decorative patterns); **b** Metallographic micrograph of M2:37-2 (from the upper right area of *Shashou* without decorative pattern); **c** Metallographic micrograph of M2:40-2 (from the upper corner edge of *Shajiao*); **d** Metallographic micrograph of M2:158-2 (from the bottom corner edge of single *Shajiao*); **e** Metallographic micrograph of M2:158-3 (from the top of single *Shajiao*); **f** Metallographic micrograph of M2:158-4 (from the middle of lower area of single *Shajiao* with decorative patterns).

forming copper oxychloride, a primary component of bronze disease, is reduced[23–25]. This environment also leads to the precipitation of Cu^{2+} and Pb^{2+} as carbonates or basic carbonates, resulting in the presence of malachite and cerussite on the surface of the bronze *Sha* and single *Shajiao*[26,27].

The corrosion of bronze can affect the results of alloy composition testing. First, different elements have varied migration abilities and behaviours during corrosion; copper and lead can form free ions and migrate out of the matrix, whereas tin tends to accumulate in situ as metal oxides[25,28]. This segregation phenomenon can influence the results of cross-sectional testing of bronzes. In energy spectrum mapping (Fig. 4), the enrichment of lead at the corroded edges of sample cross-sections and the uniform distribution of tin exemplify this type of segregation. To minimise the impact of corrosion to the greatest extent, when the energy spectrum is used for alloy composition testing, areas with severe corrosion must be avoided. Moreover, multiple measurements should be taken from several equally sized areas of the sample, and the average value should be taken thereafter. Furthermore, μXRF analysis is affected by the corrosion of the bronze, which mainly reflects the composition of the corrosion products on the surface, not the alloy composition of the artefact itself (Fig. 7). Studies have shown that XRF data from areas with thinner corrosion layers and regions with red and grey rust are more reliable, particularly where the apparent Sn concentration is the lowest[29–31]. The accuracy of the XRF data can be obtained by analyzing many points and comparing the chemical composition of different corrosion patinas to achieve statistical information about the artefact.

The analysis of the production technology of bronzes is complicated by corrosion, which is reflected in the differing sensitivities of various micrometal structures to corrosion[20,25]. The bronze *Sha* and single *Shajiao* are made through hot-working processes. Their microstructures consisted of uniformly composed equiaxed grains. These grain boundaries have higher potentials, thus becoming anodic regions that are more prone to initial corrosion[22]. Severe corrosion can lead to the destruction or loss of critical features in the microstructure, such as processing marks. For samples with severe corrosion, the etching time should not be too long when metallographic samples are prepared. The analysis of the bronze *Sha* and single *Shajiao* fabrication techniques needs to integrate various factors such as the degree of corrosion, corrosion products and corrosion processes. For example, sample M2:158-2, shown in Fig. 5d, which is severely corroded, retains only some α solid solution grains, barely visible twins, and no strain lines, but combined with the elongation and deformation of some grains and lead particles, it was analysed as a suspected hot-worked structure.

The samples are made from tin bronze or lead-tin bronze. Additionally, the contents of impurity elements are minimal, and their total contents are consistently less than 2%, indicating that the raw materials used for bronze *Sha* and single *Shajiao* are relatively pure.

Slight compositional differences are observed between different parts of the same object. For example, the sample from the right of the middle area of M2:38's left *Shajiao* is a lead-tin bronze hot-worked structure with a lead content of 3.90%; the sample from the openwork edge is a lead-tin bronze hot-worked structure with a lead content of 19.60%; and the sample from the lower middle area is a tin bronze hot-worked structure. During the hot-working process, regardless of whether the temperature is above or below the recrystallisation temperature, lead remains in a liquid or semisolid state, and under high temperatures, lead atoms move through the alloy via thermal diffusion. Thermal diffusion is a process driven by a temperature gradient, where atoms migrate from hotter regions to cooler regions, achieving redistribution[32]. Therefore, it can be inferred that during the hot-

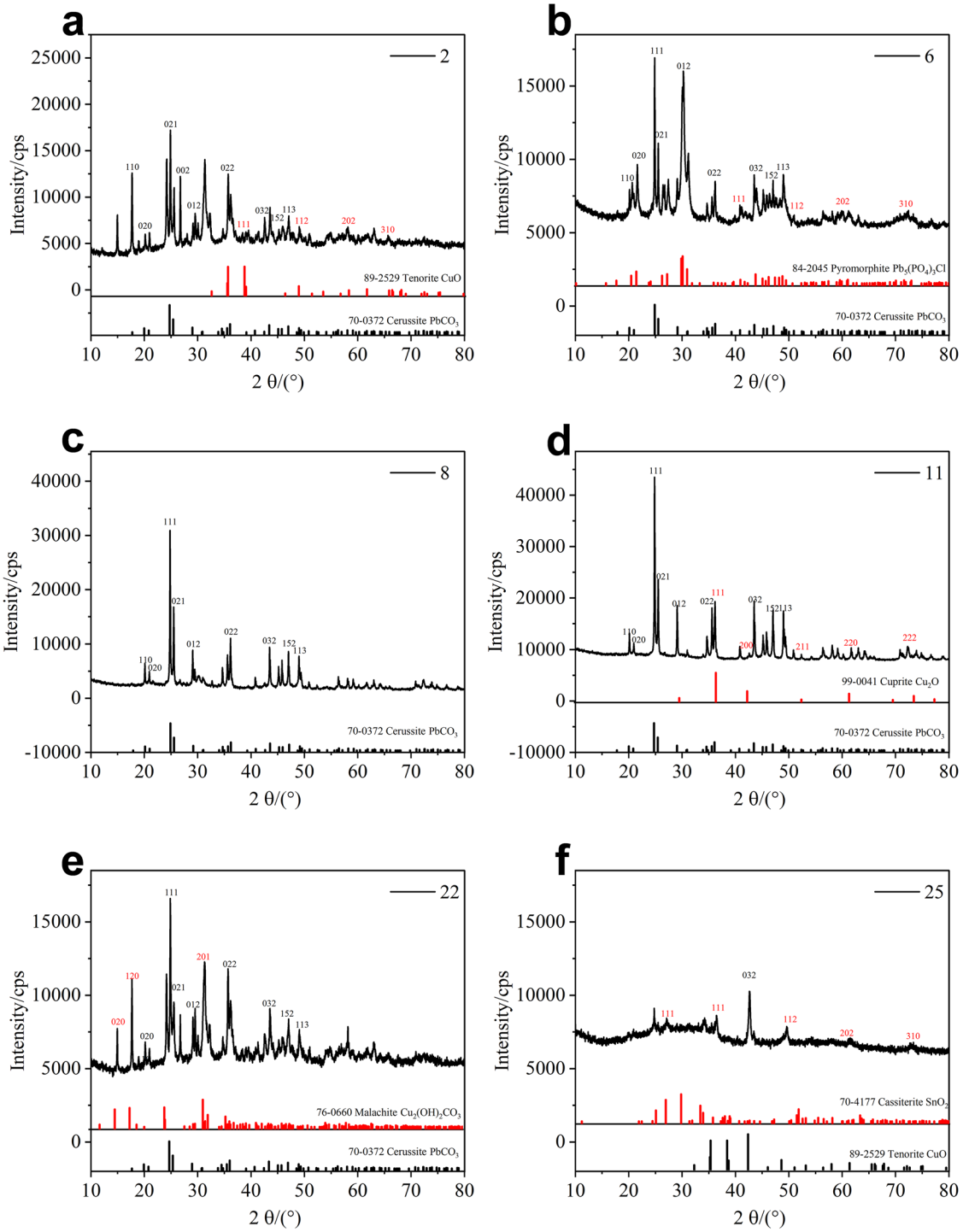

Fig. 6 | XRD spectra of bronze *Sha* and single *Shajiao* with different coloured corrosion products. a XRD spectrum of sample 2 (black corrosion of single *Shajiao* M2:58); **b** XRD spectrum of sample 6 (yellow-green corrosion of single *Shajiao* M2:41); **c** XRD spectrum of sample 8 (white corrosion of single *Shajiao* M2:41); **d** XRD spectrum of sample 11 (red corrosion of single *Shajiao* M2:158); **e** XRD spectrum of sample 22 (green corrosion of *Sha* M2:38); **f** XRD spectrum of sample 25 (grey corrosion of *Sha* M2:38).

working process, for the parts closer to the edges cool faster and at lower temperatures, leading to lead accumulation at the edges.

Ternary alloy composition plots and boxplots are drawn by categorising the samples according to different artefacts and types (shown in Fig. 8). There are significant differences in the distribution of lead content. The tin content in different parts of the same artefact also varies. Samples taken from the middle of the artefact have higher tin content than other samples. This may be due to the uneven distribution of tin content in the copper plates before hot-working. During the solidification process of casting, the presence of temperature gradients can lead to uneven redistribution of elements at the solidification front. Tin elements may enrich at the solidification front, while copper elements are repelled into the liquid phase[20]. This segregation phenomenon results in higher tin content in the central part of bronze *Sha* than in the other parts. Apart from a small number of samples at the object edges that show higher lead levels, the lead content in the remaining samples is less than 2%.

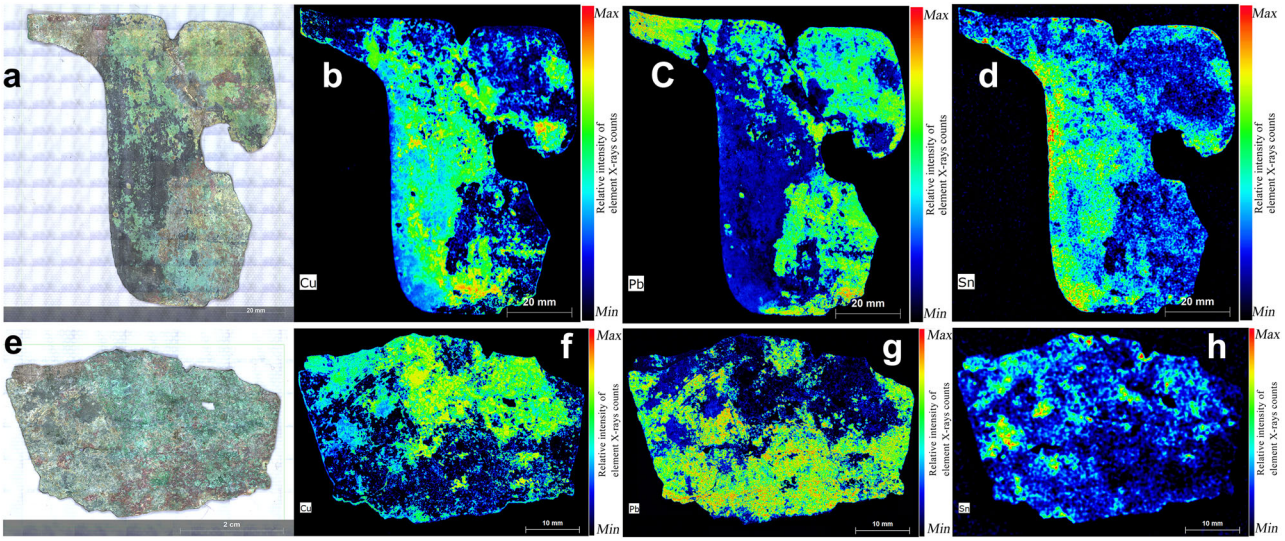

Fig. 7 | Results of μXRF mapping. a The scanning area photo of the bronze *Sha* M2:38 (corner of right *Shajiao*); **b** The Cu map of the bronze *Sha* M2:38's scanning area; **c** The Pb map of the bronze *Sha* M2:38's scanning area; **d** The Pb map of the bronze *Sha* M2:38's scanning area; **e** The scanning area photo of the bronze single *Shajiao* M2:158 (middle of the *Shajiao*); **f** The Cu map of the bronze single *Shajiao* M2:158's scanning area; **g** The Pb map of the bronze single *Shajiao* M2:158's scanning area; **h** The Sn map of the bronze single *Shajiao* M2:158's scanning area. The signal intensity is represented in a colour scale, red for the maximum and blue for the minimum (scale bar reported on the right).

An analysis of the boxplots reveals that the overall tin content in bronze *Sha* is slightly greater than that in the single *Shajiao*. This is possible because the bronze *Sha*, which includes three parts (left and right *Shajiao*, *Shagui* and *Shashou)*, requires higher support performance. Hence, a greater proportion of tin is incorporated to increase the hardness and mechanical strength of the material[33,34]. With respect to lead content, owing to the presence of outliers, the mean value is not meaningful for analysis; median values are compared instead. They have similar median values.

In an α solid solution, up to 15.8% tin can be dissolved. Bronze alloys with tin contents less than 15.8% can undergo long-duration high-temperature hot-working to eliminate eutectoid structures and achieve a single-phase α solid solution structure. While the artefact thins during hot-working, its mechanical properties improve. When the tin content is between 10% and 18% (by weight), the hardness and tensile strength are at their optimum values[35]. The late Western Zhou to early Spring and Autumn period marked the first peak in the use of hot-worked, thin-walled bronze and the formation of traditional low-tin hot-worked, thin-walled bronze technology[6]. By adding a certain proportion of tin, on the one hand, the melting point is effectively reduced, lowering the difficulty of smelting, and on the other hand, the hardness of the bronze *Sha* is increased, ensuring their support performance and shape as ritual funerary objects. As the lead content in the bronze alloy increases, both the strength and ductility significantly decrease. The lead content in hot-worked lead-tin bronzes should not be too high. Otherwise, the products are easily shattered and difficult to forge into shape[36].

Hence, the alloy compositions of the bronze *Sha* and single *Shajiao* unearthed from the Weijiaya site are clearly similar and are mostly low-tin bronzes, likely made from the same batch of materials with a stable alloy ratio, which is consistent with the traits of traditional low-tin hot-worked thin-walled bronzes crafted during the early Spring and Autumn period's formative phases. Most samples have alloy contents within a technically reasonable range, are brittle, and conform to forgeability conditions. From a metal resources perspective, the predominant low-tin bronze alloy composition of the unearthed bronze *Sha* indicates that the Qin people of that time had mastered the technology of low-tin hot-worked thin-walled bronzes. They were able to rationally select and match different metal elements based on available resources to achieve optimal alloy performance. The generally low lead content further underscores the strictness of raw material selection and the fine-tuning of alloy performance.

The samples analysed all employed hot-working techniques, allowing for a preliminary conclusion that the bronze *Sha* and single *Shajiao* unearthed from the Weijiaya site in the early Spring and Autumn period are produced via the same process.

Metallographic observations indicated that different parts of the same object may have undergone varying degrees of hot-working. For example, the samples of M2:38 all exhibit hot-working microstructures (as shown in Fig. 9). The sample from the right of the middle area has the finest grains, followed by the middle section of the lower segment, whereas the grains are the largest at the hollowed edge, indicating that the sample has undergone hot-working treatment. However, recrystallisation is incomplete because of insufficient heating time, inadequate heating temperature, or insufficient forging. We assumed that the sample from the right of the middle area was in the middle of the object, with the hot-working process moving from the centre towards the edges; hence, there was a greater amount of processing near the middle than at the edges.

Comparing the sample from the decorative area in the middle lower part of bronze *Sha* M2:37 with the sample from the undecorated area in the upper right part, the two compositions are almost identical. Both samples show α recrystallised grains and twins, with very few strain lines, indicating hot-working structures (as shown in Fig. 5a, b). However, the grains in the lower middle part with decoration are more fragmented than those in the upper right part without decoration. This suggests that this is related to the hot-working process in the decorated area, where a greater amount of processing has occurred. The four samples from bronze *Sha* M2:39 have similar grain sizes and high similarity in metallographic structure, likely because the sampling areas are all from the central parts of the objects.

All the samples of the single *Shajiao* M2:41 have similar compositions and exhibit α solid solution crystals and twins, indicating hot-working structures. The middle part of the lower section sample and the corner edge sample both have a small number of strain lines, which are signs of cold working. These signs are likely related to the sampling positions in areas with engraved decorations.

The lower bending area and upper corner edge samples of the single *Shajiao* M2:40 show numerous strain lines indicative of hot-worked and cold-worked structures. The lower bending area sample is located at a 90-degree bend at the lower part of the single *Shajiao*, suggesting that it is formed by cutting and bending after hot-working, thus showing cold

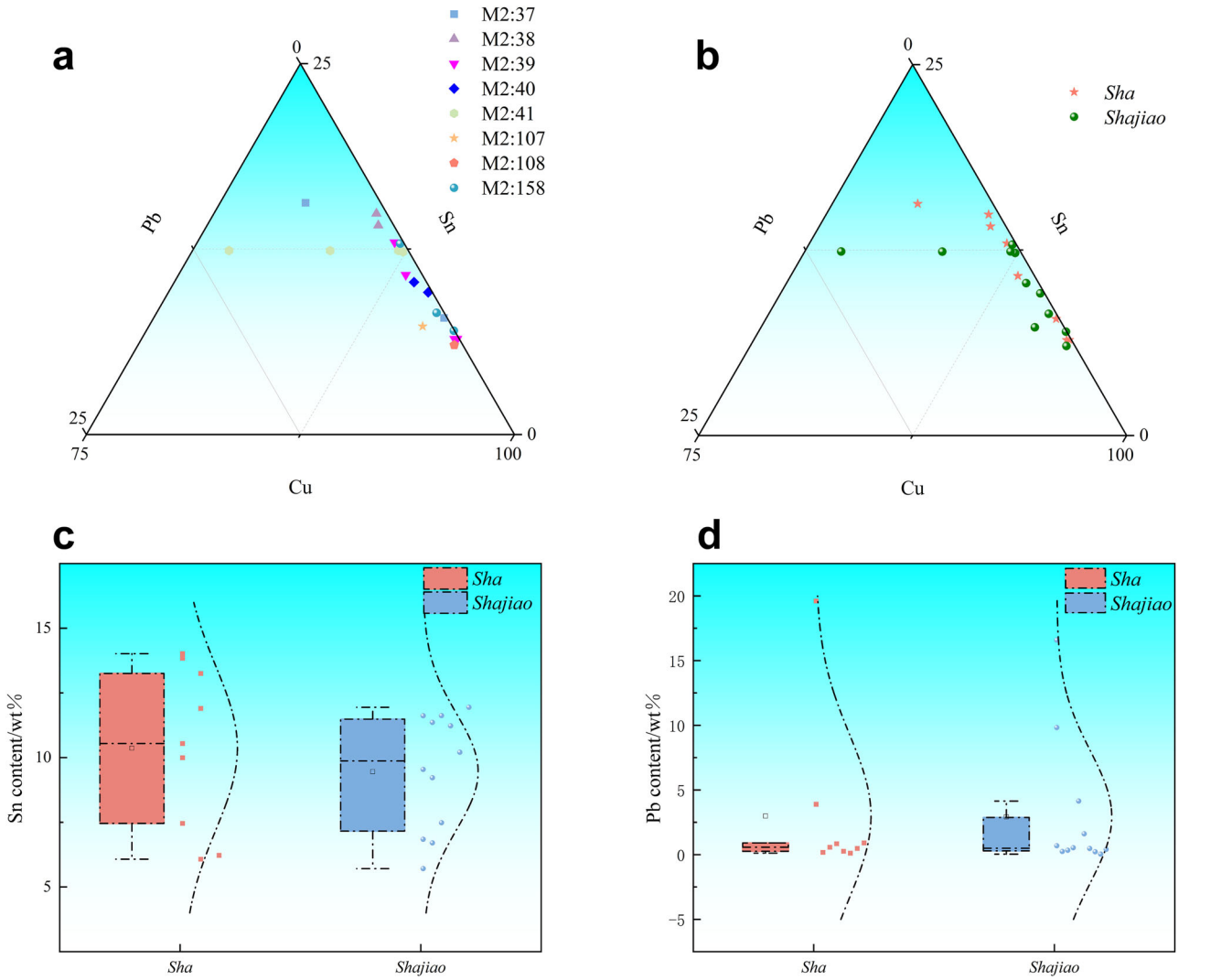

Fig. 8 | Ternary scatter plots of alloy composition and boxplots of elemental content for different types of bronze *Sha* and single *Shajiao*. **a** Ternary scatter plot of alloy composition; **b** Ternary scatter plot of alloy composition (categorised by different artefact shapes); **c** Boxplot comparison of Sn content in bronze *Sha* and single *Shajiao* (categorised by different shapes); **d** Boxplot comparison of Pb content in bronze *Sha* and single *Shajiao* (categorised by different shapes).

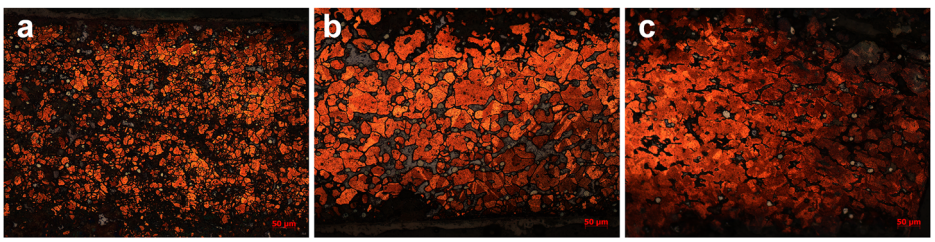

Fig. 9 | Metallographic micrographs of M2:38's samples. **a** Metallographic micrograph of M2:38-1 (from the right of middle area); **b** Metallographic micrograph of M2:38-3 (from the middle of the lower area); **c** Metallographic micrograph of M2:38-2 (from the edge of hollowed-out area).

working traces. The sample from the upper corner edge is likely shaped by cutting, thus also showing cold working traces.

From both the bronze *Sha* and single *Shajiao* perspectives, the grain size is larger, and the amount of processing is smaller at the edges, suggesting that hot-working may have been done from the centre towards the edges. Additionally, samples from areas with wide ribbon-like decorations show greater processing than those from undecorated areas, and samples from areas with engraved lines all exhibit signs of cold-working.

The hot-working of cast bronze alloys can eliminate casting defects, thus densifying the structure and improving the mechanical properties[32]. A small amount of lead in the artefacts can increase metal fluidity and reduce shrinkage during solidification. Bronze *Sha* are thin bronze sheets. Adding lead can reduce issues such as shrinkage porosity and sand holes, ensuring the aesthetic appearance of bronze *Sha*. For this reason, craftsmen consider alloy ratios and processing techniques to ensure good mechanical properties in the production of these ritual funerary objects.

The surfaces of both the bronze *Sha* and single *Shajiao* feature impressed decorations. Apart from the grooved sections, the surfaces on either side are relatively smooth, showing no signs of localised hammer marks typically seen with tool use (Fig. 10). Additionally, the decorative layouts of different bronze *Sha* and single *Shajiao* are roughly consistent in style and size when they are located at the same positions. Unearthed hot-

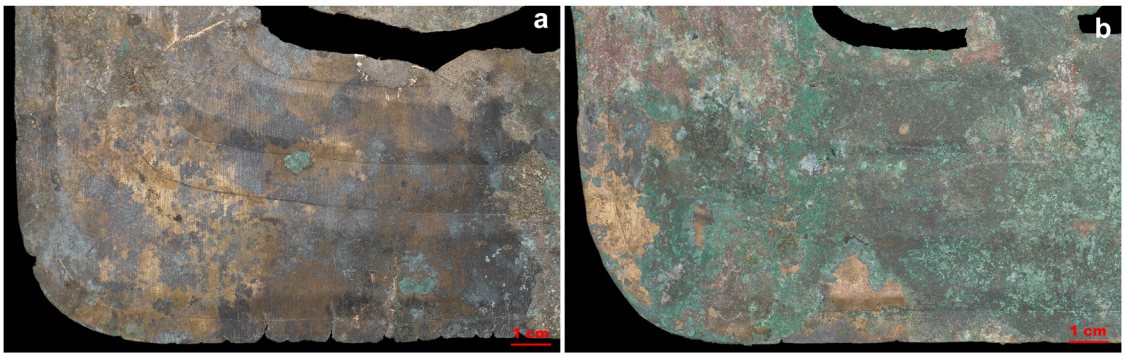

Fig. 10 | Images of the impressed decorative details. a Image of M2:40's corner; **b** Image of M2:40's corner.

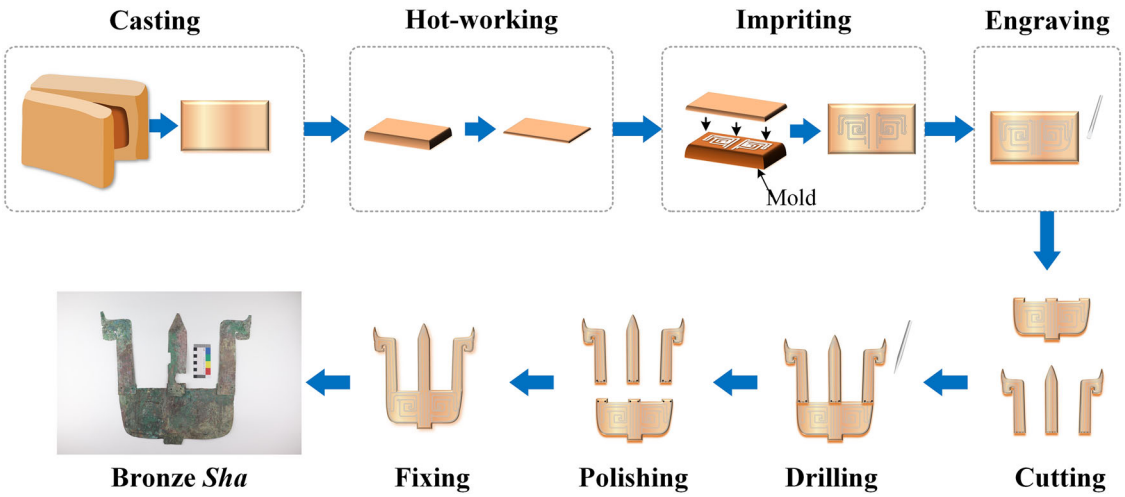

Fig. 11 | The schematic diagram of the bronze *Sha*'s production process.

working bronzes in China that use mould-pressing technology are relatively rare. Currently, they have been discovered only at the Jinsha site of Chengdu; and the Dahekou and Songjia sites of Shaanxi[37]. The impressed decorative details on Weijiaya bronze *Sha* and single *Shajiao* are similar, suggesting that the decorated areas on them are likely produced using moulds, possibly made of hardwood or other materials with similar mechanical properties. By pressing, the metal sheet covering the mould deformed to form raised decorative bands.

At the central groove of the wide decorative bands, engraved line traces are observed. The lines intersect at the turns. The starting points of the lines are either sharp or bluntly rounded. Similar engraved traces are also found on the back, indicating that these areas have undergone processing and refinement on both sides. Clear bends and pauses are observable at the junctions of the patterns; due to uneven force application by the craftsmen during the engraving process, especially at the corners (as shown in Fig. 3a).

In addition to mould pressing and engraving marks, other related technical traces are observed on this batch of bronze *Sha* and single *Shajiao*. For example, some edge positions show cutting marks (as shown in Fig. 3d). The entire surfaces of bronze *Sha* and single *Shajiao* exhibit distinct polishing lines that are arranged neatly, almost uniformly spaced, and finely detailed (as shown in Fig. 3b).

The *Shashou*, *Shagui*, left and right *Shajiao*, and some single *Shajiao* have nearly circular rivet holes, with the surrounding metal recessing towards the back. Some rivet holes are close to the decorated areas, with adjacent decorations showing signs of deformation, and some decorations are directly interrupted by the rivet holes (as shown in Fig. 3c). This suggests that the punching of the rivet holes is performed after the main decorations are made. Measurements of the diameters of the holes in the bronze *Sha* and single *Shajiao* are shown in Supplementary Data 4: Table S4. As seen in the table, apart from M2:37, the diameter range of rivet holes in each bronze *Sha* and single *Shajiao* is between 0.6 and 1.5 mm, with minimal error, and the holes are nearly perfectly circular. These findings suggest that they are formed by punching with a nearly circular-sectioned punch. Additionally, overlapping the rivet holes of *Shashou* with those of *Shagui* and *Shajiao* of the same group of bronze *Sha*, shows that the arc and cracks of the metal recessing toward the back are roughly consistent. From these traces, it can be inferred that *Shashou*, *Shagui* and *Shajiao* are stacked and punched simultaneously to ensure their stability when bound together.

From these observations, a general outline of the production process for the bronze *Sha* and single *Shajiao* unearthed from the Weijiaya site during the early Spring and Autumn period can be surmised. A schematic diagram of the bronze *Sha* production process is shown in Fig. 11.

First, the thin bronze sheets were repeatedly forged and annealed to achieve a thickness of ~0.1 cm. These were then covered over moulds made of hardwood or similar materials, imprinting the main decorative bands and forming the initial outlines of the decorations. Hard chisels were then used to carve grooves along the edges and centres of the decorative bands, enhancing the depth and artistic expression of the decorations. Subsequently, similar chisels were used to cut away the excess parts between the decorations, forming openwork while preserving necessary connections. The overall outline cutting of the bronze *Sha* was likely similar. Finally, a nearly circular-sectioned punch was used to form the rivet holes on the front. The surfaces and cut areas were then polished to enhance their aesthetic appearance and usability, presenting the final bronze *Sha* with a high level of artistry and craftsmanship.

Currently, scientific analysis data for bronze *Sha* are scarce and are mainly available from the Liujiawa site in Shaanxi, China, and the Yangshe Cemetery in Shanxi, China, where bronze *Sha* were unearthed (the

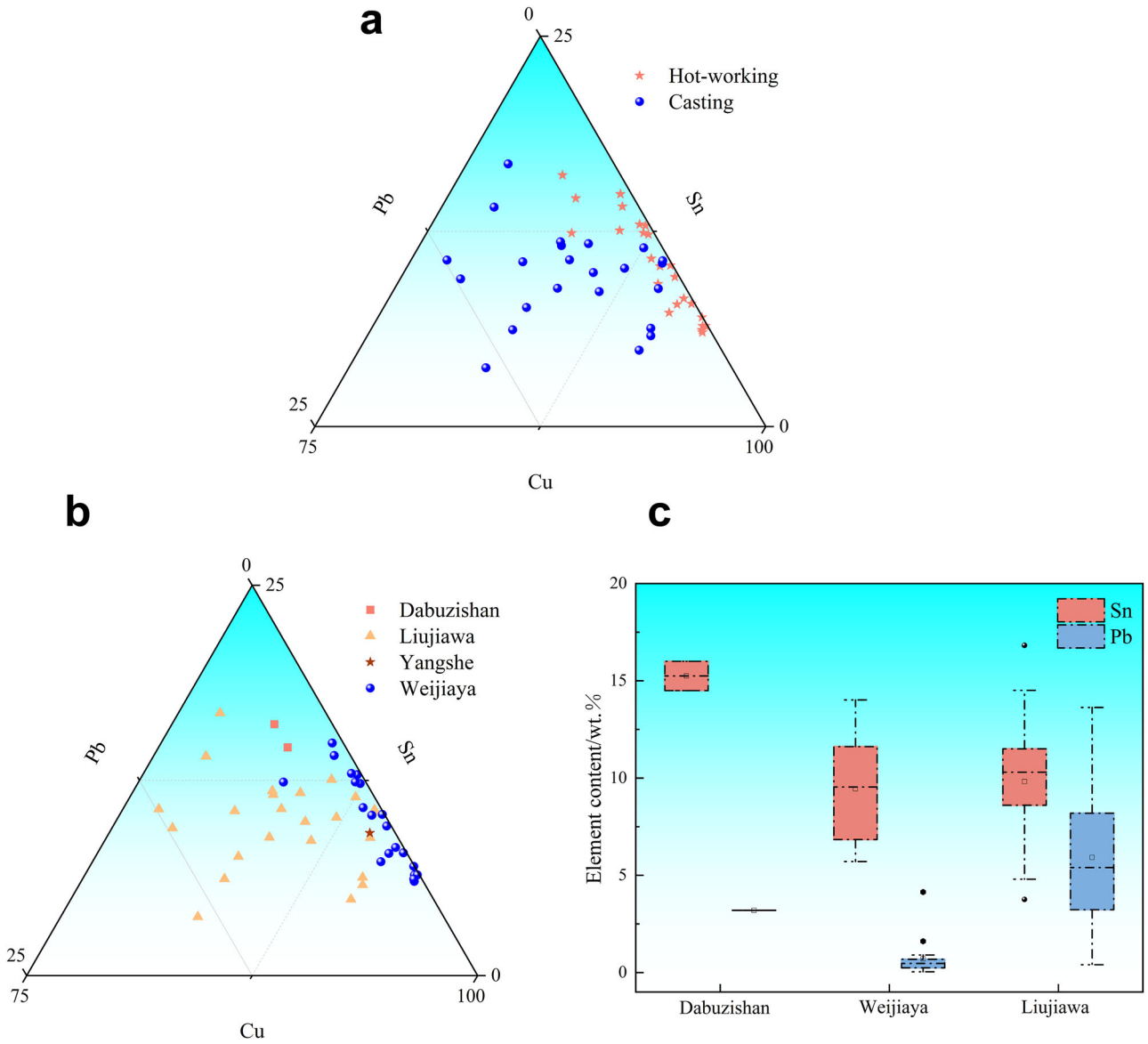

Fig. 12 | Ternary scatter plots of alloy composition and boxplot of bronze *Sha* unearthed from different sites. a Ternary scatter plot of alloy composition by different manufacturing processes; **b** Ternary scatter plot of alloy composition by different sites; **c** Boxplot comparison of Sn and Pb content by different sites.

unearthed coffin decorations from the Dabuzishan site in Gansu, China, are presumed to be bronze *Sha*)[3–5,38]. The collected data are listed in Supplementary Data 5: Table S5.

To explore the similarities and differences in the material properties of bronze *Sha* produced by different techniques, ternary alloy composition scatter diagrams were created, as shown in Fig. 12a. The analysis from the diagrams shows that most hot-worked bronze *Sha* are made of tin bronze, whereas most cast bronze *Sha* are made of lead-tin bronze, with lead content uniformly distributed between 3 and 15%. Both types have a similar range of tin content, centred at ~15%, with the majority of bronze *Sha* having a tin content greater than 5%. The addition of tin reduces the difficulty of metal smelting and increases hardness, ensuring the structural integrity of the bronze *Sha*.

The analysis indicates a strong correlation between the manufacturing techniques and the alloying materials used for bronze *Sha*. Both cast and hot-worked bronze *Sha* have tin contents of approximately 5–10%, which is technically reasonable and aligns with the bronze smelting technology characteristics of the Spring and Autumn period. For hot-worked bronze *Sha*, a lower lead content avoids the risk of matrix tearing due to the deformation of lead during hot-working.

To classify bronze *Sha* by excavation site for comparative analysis, the ternary phase diagram and boxplot are shown in Fig. 12. The diagrams reveal that the tin content and its variability at the Weijiaya and Dabuzishan sites are quite similar, with greater variability at the Liujiawa site than at the other sites. The tin content of bronze *Sha* from the Yangshe site is similar to that of the other sites. In terms of lead content, the variability and levels are greater at the Liujiawa site than at the other sites. Boxplots show that the overall lead content is highest at the Liujiawa site, followed by the Dabuzishan site, with the lowest lead content at the Weijiaya site and Yangshe site.

The Dabuzishan and Weijiaya sites are both early Spring and Autumn period Qin noble tombs. They contained bronze *Sha* made from hot-worked tin bronze, categorised within the low-tin hot-worked range of bronze, with a tin content near the highest ductility limits of the low-temperature forging zone. This finding indicates that during the early Spring and Autumn period, the Qin people mastered the technology of low-tin bronze hot-working and applied it to the production of bronze *Sha*. The Yangshe site, an early Spring and Autumn period Jin noble tomb, contained bronze *Sha* also made from tin bronze hot-working, with alloy compositions and fabrication techniques broadly consistent with those found at the

Fig. 13 | The distribution of unearthed hot-worked thin-walled bronzes. 1. Xishan site, Gansu; 2. Dabuzishan site, Gansu; 3. Weijiaya site, Shaanxi; 4. Shigushan site, Shaanxi; 5. Kongtougou site, Shaanxi; 6. Yujiawan site, Gansu; 7. Liujiawa site, Shaanxi; 8. Wayaopo site, Shanxi; 9. Yangshe site, Shanxi; 10. Zhaoxiang site, Hubei; 11. Yugang site, Hubei; 12. Qiaojiayuan site, Hubei; 13. Wenfengta site, Hubei; 14. Xiaxiangpu site, Henan.

Dabuzishan and Weijiaya sites. This shows that the Jin region also mastered the technology of hot-worked bronze *Sha*.

Scholars have found that the Zhou people of the Western Zhou period were proficient in tin bronze hot-working technology through analyses of bronze artefacts from sites such as the Yujiawan cemetery, Shigushan cemetery and Kongtougou sites[9,37]. The Liujiawa Western District site in Chengcheng, Shaanxi, China, is a Spring and Autumn early to middle period cemetery for Rui state commoners and minor nobility. This site unearthed bronze *Sha* that was cast, except for one forged piece (M21:14). During the transition between the Western and Eastern Zhou, the influence of the Zhou royal family over the vassal lords gradually weakened. The Zhou royal family and some Ji-surnamed vassal states moved east out of the Guanzhong area of Shaanxi, but the Rui state retained "remnants of the Zhou people"[39]. The casting technology and tradition of their bronze *Sha* were likely inherited from the Zhou people. Moreover, the hot-worked bronze *Sha* unearthed at Liujiawa also demonstrated that the Rui state mastered the technology of low-tin bronze hot-working. However, they primarily utilised casting for their bronze *Sha* because of the social status associated with the tombs.

No cast bronze *Sha* was unearthed in early Qin cultural sites until now. These findings suggest that the early Qin people tended to use hot-working technology in the production of bronze *Sha*. Simultaneously, the quantity of hot-worked bronze *Sha* unearthed in Henan, Shandong and Shanxi demonstrates the widespread diffusion of hot-working technology.

From the perspective of tomb status, bronze *Sha* unearthed from the Liujiawa site belonged primarily to tombs of commoners and minor nobility. Compared with those from high-status noble tombs such as Weijiaya and Dabuzishan, the tin and lead contents of these bronze *Sha* show significant variability. This difference indicates that the Rui state, represented by the Liujiawa site was less capable of obtaining metal resources than the other two states were. Additionally, hot-worked bronze *Sha* were mostly unearthed from high-status noble tombs, and only one hot-worked *Sha* was found at Liujiawa, further suggesting a connection between the emergence of hot-worked bronze *Sha* and the social status of the tomb occupants.

The Weijiaya site, as the likely location of Qianweizhihui, provides valuable physical evidence for studying the origins and development of Qin culture. The late Western Zhou and early Spring and Autumn period marked a critical period in the formation of Qin culture. During the middle Western Zhou and earlier times, hot-worked, thin-walled bronzes began to appear, and the Spring and Autumn period coincided with their popular era, with the tradition of hot-worked, thin-walled bronze craftsmanship becoming increasingly refined.

The distribution of unearthed hot-worked, thin-walled bronzes is shown in Fig. 13. The Western Zhou royal domain was the direct territory of the Zhou royal family. The Qin, Jin, Rui, Zeng, Chu and E states were among the vassal states enfeoffed by the Zhou royal house[6]. The unearthed hot-worked, thin-walled bronzes from the Xishan, Dabuzishan and Weijiaya sites belong to the Qin State, dating from the late Western Zhou period to the early Spring and Autumn period. Hot-worked, thin-walled bronzes from Shigushan, Yujiawan and Kongtougou sites belong to tombs of the Western Zhou royal domain, with Shigushan and Yujiawan sites dating from the early to middle Western Zhou period, and Kongtougou site from the late Western Zhou period. Hot-worked, thin-walled bronzes from the Liujiawa site belong to the Rui state and span the early to middle Spring and Autumn period. Those from the Wayaopo and Yangshe sites belong to the Jin state, with the Wayaopo site dating to the middle Spring and Autumn period and the Yangshe site to the late Western Zhou period. Hot-worked, thin-walled bronzes from Zhaoxiang, Yugang, Qiaojiayuan and Wenfengta sites are from the late Spring and Autumn period. The Zhaoxiang site is attributed to the Chu state, while the Wenfengta site belongs to the Zeng state. The hot-worked, thin-walled bronzes unearthed from Xiaxiangpu site belong to the E state during the late Western Zhou period[3–6,9,22,40,41]. To ensure the precision and credibility of data collection, this study has conducted a meticulous

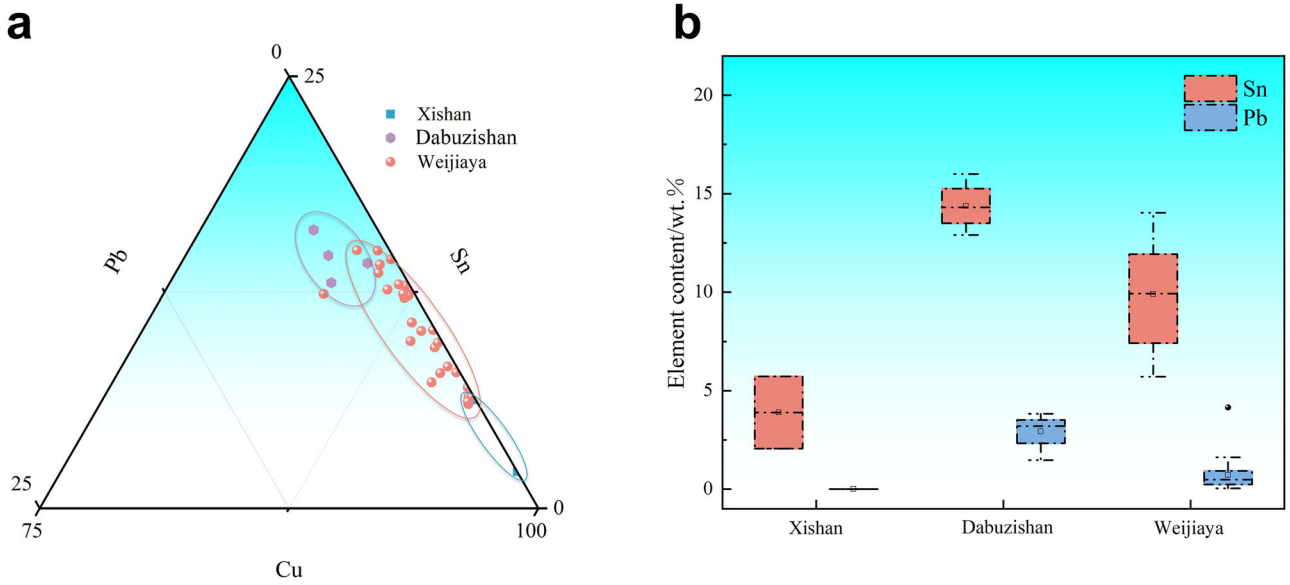

Fig. 14 | Ternary scatter plot of alloy composition and boxplot comparison of Sn and Pb content for hot-worked, thin-walled bronzes unearthed from various sites of the early Qin culture. a Ternary scatter plot; **b** Boxplot comparison of Sn and Pb content.

screening process for the data from peer-reviewed publications. First, we select samples that have a clear provenance and time of discovery, and strictly conform to the definition of hot-worked thin-walled bronzes, ensuring the accuracy of the samples' historical background. Next, we further screened samples that included both metallographic microanalysis and alloy composition analysis data. Finally, we meticulously documented the testing instruments and conditions used for each sample and summarised this detailed information in Supplementary Data 5: Table S5. The data compiled in this paper rely on scientific testing methods, appropriate testing equipment, and strict testing standards, thereby ensuring the precision and referential value of the data.

The Xishan, Weijiaya and Dabuzishan sites are important sites of early Qin culture. First, a comparative analysis of hot-worked thin-walled bronzes from different early Qin cultural sites was conducted, and ternary alloy composition scatter diagrams and boxplot of the Sn and Pb content are created, as shown in Fig. 14.

The data reveal that the dispersion of the alloy composition at the Weijiaya site is slightly greater than that at the Dabuzishan site. The lead and tin contents at the Dabuzishan site are significantly greater than at the Weijiaya site. The Dabuzishan site dates from the late Western Zhou to the early Spring and Autumn period and is presumed to be Qin royal tombs, whereas the Weijiaya site is considered a tomb of Qin nobility. The differences in alloy composition between these sites may be due to their different statuses. Compared with the other two sites, the Xishan site has a significantly different alloy composition, with extremely low alloy content. Typically, unearthed early Qin cultural sites produce hot-worked, thin-walled bronzes with low lead content, consisting of low-tin bronze, whereas bronzes unearthed at Xishan are nearly pure copper.

The analysis suggests that the material properties of hot-worked, thin-walled bronzes from different early Qin cultural sites are strongly correlated with the tomb's status and era. From a historical perspective, the Xishan site belongs to the late Western Zhou period. During the reign of King Li of Zhou, the Xirong tribes frequently raided the borders. After King Xuan of Zhou ascended to the throne, he dispatched Zhong Qin and Duke Zhuang of Qin to repel the Xirong incursions. From then on, Qin was in constant conflict with Xirong, which did not cease until the late Spring and Autumn period under Duke Wu of Qin[39]. During the late Western Zhou, a period marked by fierce clashes with Xirong, the Qin people had limited resource acquisition capabilities, which might explain why the Xishan site yielded hot-worked, thin-walled bronzes with very low alloy contents. In the early to middle Western period, the Qin power had not yet fully developed since the Xishan site was in a remote area with little interaction with the Central Plains area. At this time, the Qin bronze handicraft industry was relatively backwards, and they might not have fully mastered the low-tin bronze hot-working technology. Alternatively, it is possible that during this period, the Qin state did not have a tradition of using hot-worked, thin-walled bronzes. From late Western Zhou through the Spring and Autumn period, as Qin gradually gained the upper hand in its conflicts with Xirong and expanded eastwards into the Guanzhong area of Shaanxi, bronze production technology rapidly developed. The findings from the Dabuzishan and Weijiaya sites confirmed that, by the early Spring and Autumn period, the Qin had systematically mastered low-tin bronze hot-working technology. The alloy content of hot-worked thin-walled bronzes from the Dabuzishan site is slightly higher than that from the Weijiaya site, and its geographical position at the edge of the core area did not result in less metal resource acquisition. This suggests that the area around Dabuzishan, as well as the Xiquanqiu area, has always been a stable base for the eastward expansion of Qin and continuous growth without being neglected as the Qin power has shifted eastwards. Moreover, the tomb status at the Dabuzishan site is greater than that at the Weijiaya site, reflecting clear hierarchical differences among the Qin people.

To analyse the similarities and differences in the production techniques of hot-worked, thin-walled bronzes and to examine the cultural and technological interactions among the Qin state, the Western Zhou royal domain, and other vassal states during the Zhou Dynasties, ternary scatter diagrams and boxplots comparing the alloy compositions and Sn and Pb content are created, as shown in Fig. 15.

For discussion, we divide this period into two segments: from the Western Zhou to the middle Spring and Autumn period, and the late Spring and Autumn period. The main producers of hot-worked thin-walled bronzes during the Western Zhou to middle Spring and Autumn period were from the Qin state, the Western Zhou royal domain, the Rui state, the E state and the Jin state, whereas those from the Chu and the Zeng states date to the late Spring and Autumn period.

From the diagrams in Fig. 15, it is evident that the tin content variability is most pronounced for the Qin state, followed by the E state, with the Western Zhou royal domain and the Rui state showing similar levels of dispersion. There are too few samples from Jin state to discuss their

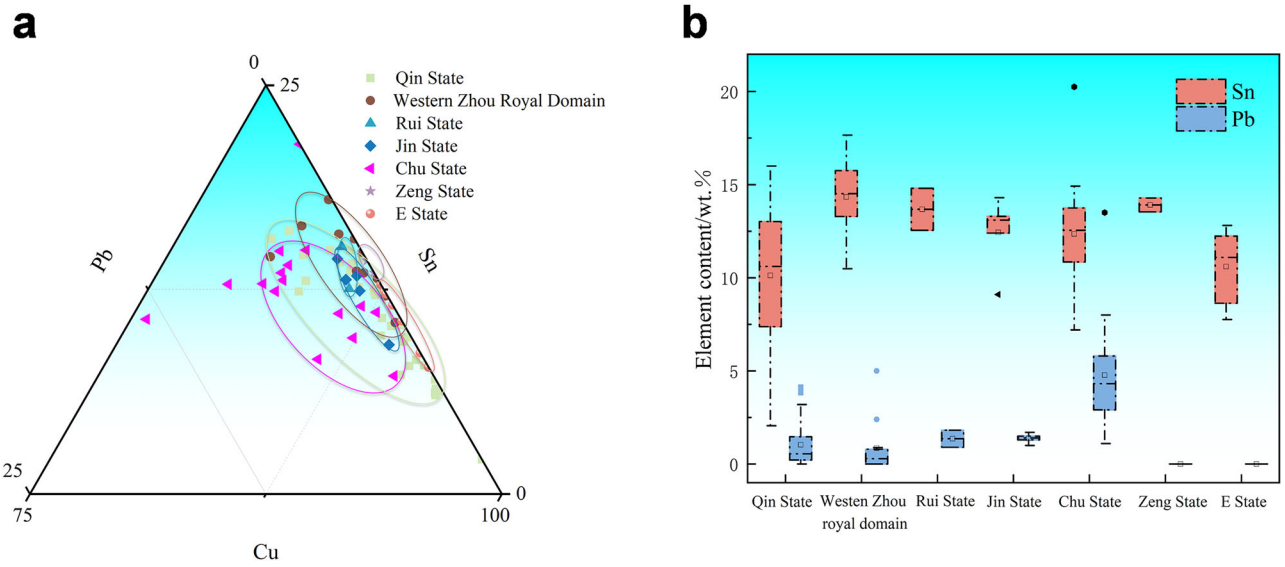

Fig. 15 | Ternary scatter plot of alloy composition and boxplot comparison of Sn and Pb content for hot-worked, thin-walled bronzes from the Qin state, the Western Zhou royal domain and other vassal states. a Ternary scatter plot; **b** Boxplot comparison of Sn and Pb content.

dispersion. The tin content is slightly higher in the Western Zhou royal domain and slightly lower in the Qin. In terms of lead content, Qin state shows slightly greater dispersion than the other states do.

First, as the centre of bronze culture at the time, the hot-worked, thin-walled bronzes of the Western Zhou royal domain had high-tin content, low lead content, and low data dispersion, reflecting the high standards and uniformity of Zhou's bronze-making technology. Zhou's technological advantage not only stemmed from their control over resources but also benefited from their central cultural and political position, allowing them to promote their technology and culture, influencing neighbouring states effectively.

Second, Qin's hot-worked, thin-walled bronzes show the lowest variability in tin content, with slightly greater variability in lead content than other states, possibly related to Qin's rapid expansion[41]. As Qin moved eastwards into the Guanzhong area of Shaanxi, it absorbed a large amount of Zhou technology and resources in a short period of time[42]. Simultaneously, as their power rapidly expanded, the increase in political and military demands might have prompted the rapid production of bronzes, potentially sacrificing some degree of technological uniformity. Additionally, from a mining and production scale perspective, Qin might have controlled the metal resources of Zhou's homeland and developed new mining and production sites. Variations in the lead and tin contents of different production batches of hot-worked, thin-walled bronzes might be due to differences in raw material sources, production conditions, etc.

Furthermore, analysing other vassal states, the Rui state, as "remnants of the Zhou" who did not leave of Guanzhong with the Zhou royal family, shows a high similarity in alloy composition with the Western Zhou royal domain, indicating that the Rui might have continued the Zhou's production techniques for hot-worked thin-walled bronzes. The high-tin content of the hot-worked thin-walled bronzes unearthed from the E state might be related to their geographical location (situated in the lower reaches of the Yangtze River, one of the most developed metallurgical areas during the Eastern Zhou period), and their mining sources and production techniques might differ from those in the Central Plains area[43–45].

Compared with hot-worked, thin-walled bronzes from the two periods, those unearthed in the late Spring and Autumn period from Chu and Zeng presented tin contents similar to those from Western Zhou to middle Spring and Autumn period but with greater variability. In terms of lead content, Chu had the highest lead content and the greatest variability. The large variability in their alloy compositions might indicate the diversity and individualised development of bronze-making technology in these states. This diversity in technical practice might stem from various interactions among states, such as cultural exchanges, the movement of craftsmen, trade, and conquests[46–48]. In summary, the production techniques for hot-worked, thin-walled bronzes during the Zhou period show a trend from a single centre to multiple developments among different states.

To further analyse the development of hot-worked, thin-walled bronzes during the Zhou dynasties, this study, in reference to Li's analysis, divides the unearthed hot-worked, thin-walled bronzes into three phases: the middle to early Western Zhou, the late Western Zhou to early Spring and Autumn, and the middle to late Spring and Autumn period. Alloy composition ternary diagrams and boxplots comparing the Sn and Pb content were created, as shown in Fig. 16[6].

The diagrams indicate that the tin content of hot-worked, thin-walled bronzes from the two Zhou periods is greater in the middle to early Western Zhou than in the middle to late Spring and Autumn period. The tin content during the middle to late Western Zhou to early Spring and Autumn period was the lowest. In terms of lead content, the middle to late Spring and Autumn period has higher levels than the other two periods do. Data dispersion is smallest in the middle to early Western Zhou, followed by the late western Zhou to early Spring and Autumn, with the largest dispersion observed in the middle to late Spring and Autumn period.

Compared with those in the other two periods, hot-worked, thin-walled bronzes from the middle to early Western Zhou period were mostly unearthed from Zhou noble tombs, with higher tin contents and lower data dispersion. This suggests that, in addition to being related to tomb status, it also relates to Zhou's control over extensive bronze resources and bronze-making technologies during this period. Furthermore, the demand for bronzes in Zhou society and a strict hierarchical system likely promoted the development of specific bronze-making techniques, with hot-worked, thin-walled bronzes from this period likely used primarily for the nobility's needs and remained relatively secretive within the Western Zhou royal domain, helping maintain their leading position in bronze making.

By the late Western Zhou to early Spring and Autumn period, hot-worked, thin-walled bronzes began appearing in high-status noble tombs of the Qin and other vassal states. As the Zhou royal house gradually declined, Qin began moving eastwards and having long resided among the Rong and Di tribes; they were more open culturally than other groups were. Facing advanced Zhou culture, they adopted an active approach in learning, absorbing, and accommodating it, which facilitated Qin's learning and utilisation of hot-worked, thin-walled bronze technology. There is another possibility that prior to their eastward expansion, the Qin state might not

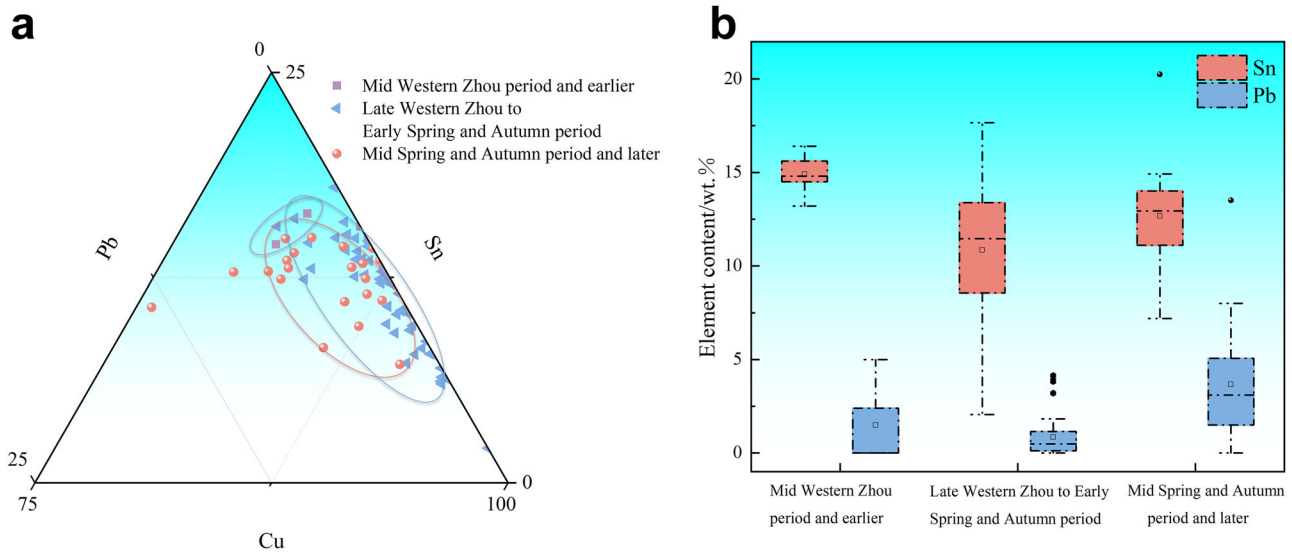

Fig. 16 | Ternary scatter plot of alloy composition and boxplot comparison of Sn and Pb content for hot-worked, thin-walled bronzes unearthed from different phases. **a** Ternary scatter plot; **b** Boxplot comparison of Sn and Pb content.

have had a tradition of using hot-worked, thin-walled bronze vessels, rather than lacking the technology itself. After moving east and being influenced by Zhou culture, they began to employ this technology in the production of such bronzes. By the late Western Zhou, Qin likely controlled significant copper resources and had the material basis for developing the bronze industry. The use of hot-worked thin-walled bronzes also became more standardised, and their numbers significantly increased. In addition to Qin, some vassal states also mastered the technology for making hot-worked thin-walled bronzes, a development likely spurred by intensified political and military competition among the states during the late Western Zhou period, promoting the development of metalworking technologies, including hot-worked thin-walled bronze production.

By the middle to late Spring and Autumn period, both lead and tin contents had increased. This period represented the peak of hot-worked thin-walled bronze popularity and the emergence of high-tin bronze hot-working systems (using tin contents above 18 wt% for hot-working)[6]. During this period, the use of hot-worked thin-walled bronzes expanded not only to high-status noble tombs of the Zhou and Qin but also to various vassal states and even middle to low-status noble and commoner tombs. As interactions among feudal states became more frequent, hot-worked thin-walled bronze technology likely spread to other regions through trade, or conquests, with the widespread adoption of production techniques representing a move towards nonstandardization. Different regions might have had different technical practices, which could be a major reason for the increased variability in alloy composition during the middle to late Spring and Autumn period. In summary, the developmental trajectory of hot-worked thin-walled bronzes during the Zhou dynasties clearly exhibited clear phase-specific characteristics and regional differences.

Through systematic scientific analysis of the early Spring and Autumn period bronze *Sha* and single *Shajiao* unearthed from the Weijiaya site in Baoji, Shaanxi, China, this study reached the following conclusions.

The analysis of corrosion revealed an uneven distribution of corrosion products such as cassiterite, cerussite, malachite, cuprite and tenorite across different areas. These corrosion characteristics directly affect the results of the alloy composition tests and the analysis of the original manufacturing techniques. We elaborate on methods to mitigate these impacts.

The microstructure and alloy composition analyses indicate that both the bronze *Sha* and single *Shajiao* were made from low-tin bronze through hot-working, involving multiple detailed processes such as shot-working, mould imprinting and engraving. This demonstrates that the Qin people had mastered the technology of low-tin hot-worked thin-walled bronzes. Compared with other unearthed bronze *Sha*, this deepens the understanding of early Qin metallurgical technology.

This study deduced the development trajectory of manufacturing technology for hot-worked, thin-walled bronzes during the pre-Qin period through a comparative analysis of hot-worked, thin-walled bronzes from different periods. The development of hot-worked, thin-walled bronzes during the early Qin cultural period was the result of technological inheritance, innovation and interactive exchanges, providing valuable insights into the interaction and development of ancient bronze civilisations.

In conclusion, through scientific archaeology, this study not only reveals the corrosion characteristics and refined manufacturing processes of the bronze *Sha* but also deepens the understanding of early Qin culture and its hot-worked thin-walled bronze production techniques and cultural exchanges. These findings provide not only important scientific evidence and new research perspectives for further exploration of the metallurgical techniques and sociocultural structure of Qin culture but also supplementary material for the historical context of the evolution of hot-worked thin-walled bronze technology.

Data availability

The datasets used during the current study are available from the corresponding author on reasonable request.

Abbreviations

XRD	X-ray diffraction
μXRF	micro X-ray fluorescence
SEM-EDS	metallurgical microscopy and scanning electron microscopy–energy dispersive X-ray spectroscopy
SDD	silicon drift detector.

Received: 4 September 2024; Accepted: 29 March 2025;
Published online: 03 November 2025

References

1. Shaanxi Academy of Archaeology, Northwest University School of Cultural Heritage. Excavation report of spot B and C of Weijiaya site, Baoji city, Shaanxi province. *Archaeol. Cult. Relics* (in press).
2. Zhang, T. E. A preliminary understanding of Zhou dynasty coffin decorations and bronze sha. *Collect. Stud. Archaeol.* **20**, 293–304 (2011).

3. Zhang, B., Xia, P. C., Yu, Y. G. & Cui, M. H. Preliminary research on the bronze sha unearthed from the western district cemetery of Liujiawa, Chengcheng, Shaanxi. *Wenbo* **40**, 91–99 (2023).
4. Shao, A. D., Sun, S. Y., Mei, J. J., Chen, K. L. & Wang, H. Scientific analysis and research on metal artifacts unearthed from the Qin duke's tomb at Dabuzishan in Lixian, Gansu. *Cult. Relics* **66**, 86–96 (2015).
5. Nan, P. H. *Research on Bronze Technology of Jin Kingdom in Spring and Autumn Period*. PhD thesis, University of Science and Technology Beijing (2018).
6. Li, Y. *Between the Forge and Hammer: A Study on the Hot Forging of Thin-Walled Bronze Ware from the Early Qin to the Han Dynasties* (Shanghai Classics Publishing House, 2017).
7. Pigott, V. C. & Goodway, M. High-tin bronze gong making: part one of two. *JOM* **40**, 36–37 (1988).
8. Qinghai Provincial Institute of Cultural Relics, School of Archaeology Archaeology, & Beijing University Museology. *Gamatai of Guinan* (Science Press, 2016).
9. Zhang, Z. G. & Ma, Q. L. Metallographic and compositional analysis of bronze artifacts unearthed from the Western Zhou tombs at Yujiawan, Gansu province. *Sci. Conserv. Archaeol.* **20**, 24–32 (2008).
10. Figueiredo, E., Valério, P., Araújo, M. F. & Senna-Martinez, J. C. Micro-EDXRF surface analyses of a bronze spearhead: lead content in metal and corrosion layers. *Nucl. Instrum. Methods Phys. Res. Sect. Accel. Spectrom. Detect. Assoc. Equip.* **580**, 725–727 (2007).
11. Pollard, A. M., Zhang, Y. & Liu, R. Bronze alloying recipes at Anyang during the Shang dynasty. *Archaeol. Anthropol. Sci.* **15**, 156 (2023).
12. Manti, P. & Watkinson, D. Corrosion phenomena and patina on archaeological low-tin wrought bronzes: New data. *J. Cult. Herit.* **55**, 158–170 (2022).
13. Ingo, G. M., De Caro, T., Riccucci, C. & Khosroff, S. Uncommon corrosion phenomena of archaeological bronze alloys. *Appl. Phys. A* **83**, 581–588 (2006).
14. Fan, X. & Freestone, I. C. Occurrence of phosphatic corrosion products on bronze swords of the Warring States period buried at Lijiaba site in Chongqing, China. *Herit. Sci.* **5**, 48 (2017).
15. Fan, X., Wang, Q. & Wang, Y. Non-destructive in situ Raman spectroscopic investigation of corrosion products on the bronze dagger-axes from Yujiaba site in Chongqing, China. *Archaeol. Anthropol. Sci.* **12**, 90 (2020).
16. Mezzi, A. et al. Unusual surface degradation products grown on archaeological bronze artefacts. *Appl. Phys. A* **113**, 1121–1128 (2013).
17. Oudbashi, O. A methodological approach to estimate soil corrosivity for archaeological copper alloy artefacts. *Herit. Sci.* **6**, 2 (2018).
18. Di Turo, F., Coletti, F. & De Vito, C. Investigations on alloy-burial environment interaction of archaeological bronze coins. *Microchem. J.* **157**, 104882 (2020).
19. Oudbashi, O. Multianalytical study of corrosion layers in some archaeological copper alloy artefacts. *Surf. Interface Anal.* **47**, 1133–1147 (2015).
20. Wang, X. et al. Mechanism of corrosion behavior between Pb-rich phase and Cu-rich structure of high Sn–Pb bronze alloy in neutral salt spray environment. *J. Mater. Res. Technol.* **29**, 881–896 (2024).
21. Pagano, S. et al. Archaeometric characterisation and assessment of conservation state of coins: The case-study of a selection of Antoniniani from the hoard of Cumae (Campania region, Southern Italy). *Heritage* **6**, 2038–2055 (2023).
22. Hu, Y. J., Zhang, B., Xia, P. C., Shao, A. D. & Chen, J. L. Study on the corrosion causes of bronze wares unearthed from the Liujiawa site in Chengcheng. *Sci. Conserv. Archaeol.* **34**, 78–87 (2022).
23. Chang, T., Maltseva, A., Volovitch, P., Odnevall Wallinder, I. & Leygraf, C. A mechanistic study of stratified patina evolution on Sn-bronze in chloride-rich atmospheres. *Corros. Sci.* **166**, 108447 (2020).
24. Hu, Y., Wei, Y., Li, L., Zhang, J. & Chen, J. Same site, different corrosion phenomena caused by chloride: the effect of the archaeological context on bronzes from Sujialong Cemetery, China. *J. Cult. Herit.* **52**, 23–30 (2021).
25. Zhao, T. et al. Corrosion of ancient Chinese bronze fragments from different periods and protective effect of menthol coating. *Corros. Commun.* **12**, 46–57 (2023).
26. Oudbashi, O., Hasanpour, A. & Davami, P. Investigation on corrosion stratigraphy and morphology in some Iron Age bronze alloy vessels by OM, XRD and SEM–EDS methods. *Appl. Phys. A* **122**, 262 (2016).
27. Boccaccini, F. et al. Reproducing bronze archaeological patinas through intentional burial: a comparison between short- and long-term interactions with soil. *Heliyon* **9**, e19626 (2023).
28. Robbiola, L., Blengino, J.-M. & Fiaud, C. Morphology and mechanisms of formation of natural patinas on archaeological Cu–Sn alloys. *Corros. Sci.* **40**, 2083–2111 (1998).
29. Robotti, S. et al. Reliability of portable X-ray fluorescence for the chemical characterisation of ancient corroded copper-tin alloys. *Spectrochim. Acta Part B At. Spectrosc.* **146**, 41–49 (2018).
30. Dussubieux, L. & Walder, H. Identifying American native and European smelted coppers with pXRF: a case study of artifacts from the Upper Great Lakes region. *J. Archaeol. Sci.* **59**, 169–178 (2015).
31. Holakooei, P., Oudbashi, O., Mortazavi, M. & Ferretti, M. On, under and beneath the patina: evaluation of micro energy dispersive X-ray fluorescence quantitative data on the classification of archaeological copper alloys. *Spectrochim. Acta Part B At. Spectrosc.* **178**, 106128 (2021).
32. Scott, D. A. & Schwab, R. *Metallography in Archaeology and Art* (Springer International Publishing, 2019).
33. Luo, Z. et al. Diversified manufacturing processes and multiple mineral sources: features of warring states bronze vessels excavated from Chutai Cemetery M1, Anhui province. *Sci. China Technol. Sci.* **66**, 2297–2307 (2023).
34. Li, Y. et al. Techniques employed in making ancient thin-walled bronze vessels unearthed in Hubei province, China. *Appl. Phys. A* **111**, 913–922 (2013).
35. Witasiak, D. et al. Effect of alloying additives and moulding technology on microstructure, tightness, and mechanical properties of $CuSn_{10}$ bronze. *Materials* **16**, 7593 (2023).
36. Chattopadhyay, P. K., Datta, P. K. & Maji, B. Forging technology of high-tin bronzes in ancient Bengal. *Curr. Sci.* **118**, 1822–1831 (2020).
37. Haichao, L. et al. Cold-worked and annealed bronze objects and relevant motif techniques in the Chinese Bronze Age: Analysis of bronze sheets found at Songjia cemetery in Shaanxi, China. *Archaeometry* **62**, 54–67 (2020).
38. Hu, Y. J. et al. Technical and resource study on the bronze wares unearthed from the eastern I district cemetery of the Liujiawa site in Chengcheng, Shaanxi. *Cult. Relics* **74**, 86–96 (2023).
39. Liang, Y. On the origins and formation of early Qin culture. *Acta Archaeol. Sin* **71**, 149–174 (2017).
40. He, Y., Huang, R. X., Liang, Q., Liu, C. & Liang, Y. A scientific analysis of the materials and techniques of bronzes unearthed from the Qin tombs during the early Spring and Autumn period in Weijiaya site, Baoji city, Shaanxi province. *Archaeol. Cult. Relics* (in press).
41. Fang, H., Feinman, G. M. & Nicholas, L. M. Imperial expansion, public investment, and the long path of history: China's initial political unification and its aftermath. *Proc. Natl Acad. Sci. USA* **112**, 9224–9229 (2015).
42. Lander, B. *Environmental Change and the Rise of the Qin Empire: A Political Ecology of Ancient North China*. PhD thesis, Columbia University (2015).
43. Li, Q. et al. Scientific analysis on the Han bronze wares unearthed from Xiangyang, Hubei province, China. *Archaeol. Anthropol. Sci.* **15**, 103 (2023).

44. Yu, Y. et al. Scientific study of bronze bells of the Western Zhou period recovered in Yichang, Hubei. *J. Cult. Herit.* **56**, 85–95 (2022).
45. Ma, J., Wu, X. & Yan, X. Metal trade and national integration: Bronze technology and metal resources of Yue style bronzes from Hunan (8 ~ 5 C. BCE). *Herit. Sci.* **11**, 128 (2023).
46. Zhang, K., Li, Q., Bai, B., He, J. & Li, H. The production of bronze weapons in the Chu state: a case study of bronze arrowheads excavated from the Yuwan cemetery in Hubei, China. *Archaeol. Anthropol. Sci.* **16**, 152 (2024).
47. Zhang, R., Wei, G. & Huang, X. Scientific analysis of the bronze artifacts excavated from Xinfeng cemetery, Lintong district, Xi'an city, China: Raw material sources determined by lead isotopes and trace elements. *Eur. Phys. J. Plus* **138**, 813 (2023).
48. Li, H. et al. Production and circulation of bronzes among the regional states in the Western Zhou dynasty. *J. Archaeol. Sci.* **121**, 105191 (2020).

Acknowledgements

Thanks to Dr. Ruiliang Liu of the British Museum for the guidance on the research direction of the thesis and academic writing. Our sincere gratitude to UCL PhD student Kangte He for the suggestions and guidance provided for the research approach of this paper. We would also like to express our thanks to Chang Liu and Runze Kou of Northwest University for their assistance in the sample collection process. This research was supported by the National Key Project Corrosion Mechanism of Bronze and Typical Bronze Diseases (Project No. 2020YFC1522001). This work was supported by the Archaeological Talent Promotion Program of China (No. 2025-187).

Author contributions

C.L. presided over the entire research and designed the overall framework of the manuscript. R.H. conducted sample collection and field analysis and was the main contributor to the writing of the paper. X.L. and Y.H. reviewed and revised the paper. Y.L. provided all the samples used in the paper, and L.X. assisted in the excavation and collection of samples. All authors read and approved the final manuscript.

Competing interests

The authors declare no competing interests.

Additional information

Supplementary information The online version contains supplementary material available at https://doi.org/10.1038/s40494-025-01676-0.

Correspondence and requests for materials should be addressed to Cheng Liu or Yun Liang.